Review Paper

Potential Aquifer Vulnerability in Regions Down-Gradient from Uranium In Situ Recovery (ISR) Sites

James A. Saunders[a], Bruce E. Pivetz[b], Nathan Voorhies[c], Richard T. Wilkin[d]

[a] Department of Geosciences, 210 Petrie Hall, Auburn University, AL 36849, United States of America

[b] CSS-Dynamac, 10301 Democracy Lane Suite 300, Fairfax, VA 22030, United States of America

[c] Environmental Solutions and Services, Battelle, 1300 Clay St., Suite 600, Oakland, CA 94612, United States of America

[d] U.S. Environmental Protection Agency, National Risk Management Research Laboratory, Ground Water and Ecosystems Restoration Division, 919 Kerr Research Dr., Ada, Oklahoma 74820 United States of America. Corresponding Author, 580-436-8874, wilkin.rick@epa.gov

August 2016
Submission to *Journal of Environmental Management*

Highlights

- Uranium ores in roll-front deposits are extracted using in situ recovery (ISR).
- Uranium roll-front deposits are comprised of a variety of trace metals.
- Aquifers may be vulnerable to contamination during or after ISR operations.
- Hydrogeochemical characterization is necessary for post-ISR aquifer restoration.

Abstract

Sandstone-hosted roll-front uranium ore deposits originate when U(VI) dissolved in groundwater is reduced and precipitated as insoluble U(IV) minerals. Groundwater redox geochemistry, aqueous complexation, and solute migration are important in leaching uranium from source rocks and transporting it in low concentrations to a chemical redox interface where it is deposited in an ore zone typically containing the uranium minerals uraninite, pitchblende, and/or coffinite; various iron sulfides; native selenium; clays; and calcite. *In situ* recovery (ISR) of uranium ores is a process of contacting the uranium mineral deposit with leaching and oxidizing (lixiviant) fluids via injection of the lixiviant into wells drilled into the subsurface aquifer that hosts uranium ore, while other extraction wells pump the dissolved uranium after dissolution of the uranium minerals. Environmental concerns during and after ISR include water quality degradation from: 1) potential excursions of leaching solutions away from the injection zone into down-gradient, underlying, or overlying aquifers; 2) potential migration of uranium and its decay products (e.g., Ra, Rn, Pb); and, 3) potential mobilization and migration of redox-sensitive trace metals (e.g., Fe, Mn, Mo, Se, V), metalloids (e.g., As), and anions (e.g., sulfate). This review describes the geochemical processes that control roll-front uranium transport and fate in groundwater systems, identifies potential aquifer vulnerabilities to ISR operations, identifies data gaps in mitigating these vulnerabilities, and discusses the hydrogeological characterization involved in developing a monitoring program.

Keywords

Uranium fate and transport; roll-front deposits; in situ leaching; trace metal mobilization; uranium geochemistry; hydrogeology; groundwater monitoring.

Introduction

In situ recovery (ISR) of uranium is an alternative to conventional mining of the element. ISR is a process of contacting a mineral deposit with leaching (lixiviant) fluids to dissolve ore minerals for recovery by groundwater extraction (Underhill, 1992; Davis and Curtis, 2007). Potentially it can cause fewer environmental consequences than traditional mining techniques, such as production of mine tailings, and can economically extract lower-grade ores due to its lower costs than conventional mining (Davis and Curtis, 2007). The first commercial-scale ISR operation (in the United States of America [US] and the world) was opened by ARCO at George West, Texas in 1975. Now ISR accounts for almost half of the world's uranium production (World Nuclear Association, 2014), and greater than 90% of the US current uranium production since about 1995 (Mudd, 2001).

The process of ISR involves the drilling of wells to inject a leaching solution into the subsurface aquifer that hosts uranium ore, and other wells to pump the dissolved uranium in the "pregnant" solutions after dissolution of the uranium minerals. Leach solutions used in the US are typically dilute and contain both an oxidizing agent and a source of carbonate to enhance uranium solubility. ISR of uranium has some similarities to salt brining operations, sulfur mining by the Frasch process, and ISR of other metals such as copper and gold (e.g., Dershowitz, 2011). Further, the process shares some of the same issues as "pump-and-treat" groundwater remediation technologies, such as the potential inefficient removal of contaminants that have diffused into finer-grained aquifer materials. Indeed, the "groundwater sweep" technique commonly used in early stages of aquifer restoration after ISR is essentially a pump-and-treat groundwater remediation technique (Deutsch et al., 1984; Catchpole and Kucheka, 1993).

Although environmental problems related to ISR of uranium in the US are not as great as those for conventional mining, there are concerns (Mudd, 2001). These include excursions of oxidizing leach solutions away from the injection zone into the down-gradient aquifer or into overlying and underlying aquifers (Deutsch et al., 1985; Staub et al., 1986). Besides uranium and its decay products (e.g., radium, radon, lead and polonium; [Ludwig, 1978]) the leaching solutions have the capacity of dissolving and mobilizing a number of trace metals and metalloids of environmental concern, including arsenic, selenium, vanadium, and molybdenum (Deutsch et

al., 1984). Monitoring wells are located up- and down-gradient of the production area to determine if an excursion occurs. Excursions are identified by monitoring changes in water level, total dissolved solids, and/or a suite of geochemical parameters and dissolved constituents (Deutsch et al., 1984). After ISR of uranium is completed, regulations in the US require water quality to be restored to pre-mining background levels (NRC, 2003; Campbell et al., 2007; Johnson et al., 2010). Aquifer restoration is complicated by anisotropic reservoir properties such as highly directional permeabilities, bedding plane discontinuities, water-rock geochemical reactions, and uranium roll front characteristics (Stover, 2004).

There has been essentially a three-decade hiatus from the 1970s to the 1990s on published detailed geologic, geochemical, and hydrogeologic studies of the uranium ores in the US amenable to exploitation by ISR. The U.S. EPA is developing new proposed standards for ISR operations at 40 CFR 192 (Federal Register, 2015). Here we present an update on the origin and nature of these ores, and their extraction by ISR. This document presents a review of the geology, geochemistry, and hydrogeology of uranium deposits (focusing on roll-front deposits in the US); the ISR process; and provides basic information on the vulnerability of down-gradient groundwater and on monitoring that may be conducted to assess this vulnerability.

2. Background: Uranium Roll-Front Deposits

Sandstone uranium deposits account for 25% of world uranium resources (Kyser, 2014), and roll-front uranium ores are one of the two most abundant classes of sandstone-hosted uranium ores (Nash et al., 1981; Kyser, 2014). Roll-front ores are arcuate bodies of mineralization that crosscut sandstone bedding. In contrast, tabular sandstone deposits, which are the other main class of sandstone uranium ores, are irregular, elongated lenticular bodies parallel to the depositional trend, commonly occurring in paleo-channels incised into underlying sediments (Finch and Davis, 1985). Roll-front deposits are the current focus of ISR mines in the US. As of early 2014, there were seven producing ISR mines and three additional ones that had been licensed and are under construction (Fig. 1). During the heyday of US uranium mining during the Cold War (1950s and 60s) there were more than 50 operating conventional mines and mills (DOE, 1995; Smith, 2011). Because of the decrease in the price of uranium in the 1970s and 1980s, all but one of those conventional mining operations is still operating, leaving

approximately 127 million metric tons of uranium mill tailings at the surface that pose an environmental threat (Krauskopf, 1988). As a consequence, the US Congress passed the *Uranium Mill Tailings Control Act of 1978,* which called for cleanup of mill tailings from abandoned uranium and other metal mines in the US (Kesler, 1994). Most current regulations require that these wastes be disposed of underground or in piles at the surface surrounded and covered by impermeable clay, flexible membrane liners, and leak-detection systems to prevent groundwater contamination (e.g., Gershey et al., 1990). Because of greatly fluctuating uranium prices, the environmental costs of dealing with conventional mining and extraction, and common lower grades of new deposits, the ISR process for uranium extraction has become increasingly important (U.S. EPA, 1995; NRC, 2009a,b). In 1979, ISR accounted for only 9% of US uranium production (Larson, 1981), but has risen to >90% since the mid-1990s (Mudd, 2001).

ISR in the US exploits sandstone-hosted roll-front uranium deposits, which are defined as epigenetic (e.g., formed after the host formation was deposited) concentrations of uranium minerals that are typically Silurian or younger in age. They occur as impregnations and replacements primarily in gently dipping permeable fluvial, lacustrine, and deltaic arkosic sandstone formations or in molasse-like sequences in fluvial–lacustrine systems in wide forelands between a subduction zone and an intracratonic sea (Nash et al., 1981; Finch and Davis, 1985; IAEA, 2009; Kyser, 2014). In particular, leachable uranium deposits are found in sandstones that have been deposited in intermontane basins, or in nearshore marine or deltaic environments (Davis and Curtis, 2007). The basins range in size from a few hundred square miles (Shirley Basin, Wyoming [WY]) to several thousand square miles (Powder River Basin, WY; southeast Texas [TX]; Harshman and Adams, 1980; see Fig. 1). The deposits occur in medium- to coarse-grained sandstones bounded by relatively impermeable shale/mudstone units that are interbedded in the sedimentary sequence and normally lie just above and below the mineralized sandstone (Kyser, 2014). Uranium precipitated to form crescent-shaped ore bodies in cross section that are convex in a down-gradient direction. Individual ore bodies rarely exceed a few hundred meters in length, commonly being a few tens of meters wide and 10 meters or less thick (Davis and Curtis, 2007). Uranium ores apparently precipitated under reducing geochemical conditions, which were caused by one or more of a variety of reducing agents within the sandstone, including carbonaceous material (detrital plant debris, amorphous humate,

and marine algae), sulfides (pyrite and H_2S), hydrocarbons (petroleum and methane), and interbedded mafic volcanics (Nash et al., 1981; IAEA, 2009; Kyser, 2014). Roll-front deposits are commonly low to-medium grade (0.05–0.4% U) and individual ore bodies are small to medium in size, ranging up to a maximum of 50,000 metric tons U (Kyser, 2014). Typically organic reductants occur as detrital material in the un-altered sandstones, but locally were also introduced by faults from deeper zones, such as in the southeast Texas roll-front ores (Galloway, 1978; Goldhaber et al., 1978; Reynolds et al., 1982; Reynolds and Goldhaber, 1983).

Current models (Kyser and Cuney, 2008; IAEA, 2009; Kyser, 2014) for roll-front uranium deposits emphasize that ores precipitated from oxidized groundwater. The redox geochemistry and migration of these groundwaters are instrumental in leaching uranium from source rocks and transporting it in low concentrations to a chemical redox interface where it is deposited. Essential parameters that control these processes include depositional environment, host rock lithology and permeability, adsorptive/reducing agents, groundwater chemistry amenable to leaching and transporting uranium, and a source of uranium (IAEA, 2009). The presence of uraniferous tuffaceous material either as a constituent of the host sandstone or in adjacent strata may enhance the favorability of a fluvial system, due to its potential as a uranium source rock (Walton et al., 1981). Felsic (e.g., silica-rich) volcanic and crystalline terrains are also considered to be potential uranium source rocks for roll-front uranium deposits (IAEA, 2009). The feldspar component of the host rocks, though probably of no direct importance in the mineralizing process, indicates a granitic source from which the uranium may have originated and an environment of rapid erosion and sedimentation providing the required hydro-physical conditions such as permeability needed for adequate groundwater migration. Impermeable or less permeable strata or other barriers may be instrumental in vertically and laterally channeling uraniferous fluids to favorable sites of uranium deposition, while at the same time prohibiting widespread flushing and dilution of fluids (IAEA, 2009).

3. Mineralogy, Geochemistry, and Genesis of Roll-Front Uranium Deposits

The environmental chemistry of uranium in aquatic environments has been reviewed in previous reports (e.g., Langmuir, 1997; Fanghanel and Neck, 2002). This section is intended to provide an overview of the processes that control uranium transport and fate in groundwater

systems. In nature, uranium occurs in the oxidation states U^{+4}, U^{+5}, and U^{+6}; however, most uranium geochemistry can be described in terms of the reduced form, U^{+4}, and the oxidized form, U^{+6} (Fanghanel and Neck, 2002). Uranium is the heaviest naturally occurring element and all of its isotopes are radioactive. Natural uranium comprises three isotopes: ^{238}U ($4.468x10^9$ year half-life) and ^{235}U ($7.038x10^8$ year half-life) account for 99.285 and 0.71 percent of the element's natural abundance, respectively. The radiogenic daughter ^{234}U ($2.445x10^5$ year half-life) makes up the remainder (0.005%). Recent studies have shown that natural ^{236}U can also be produced in groundwater near high-grade uranium ores by neutron capture on ^{235}U (Murphy et al., 2015). Atoms of these uranium isotopes have heavy nuclei and their ions have large ionic radii (0.66-1.14 Å).

Groundwater concentrations of dissolved uranium are usually on the order of a few micrograms per liter (µg/L), but can range to as high as 50,000 µg/L in areas near uranium tailings sites (Abdelouas et al., 2000). For comparison, the concentration of uranium in seawater is about 3 µg/L (Mann and Wong, 1993). In addition to the dissolved forms, colloidal forms of uranium are often present in surface water and groundwater, and can be assessed using ultrafiltration methods (Giblin et al., 1981; Guo et al., 2007). The U.S. EPA has established the Maximum Contaminant Level (MCL) for uranium at 30 µg/L.

Uranium transport in groundwater depends mainly on the oxidation state and radioactive decay phenomena for the predominant radioisotopes found in natural systems. In water, uranium has a strong tendency to bond to oxygen to form soluble oxyions. Under highly acidic and reducing conditions, the uranous cation (U^{4+}) can occur in solution, or it can combine with fluoride to form a complex (e.g., UF^{3+}, UF_2^{2+}). At acidic to alkaline pH, the uranous ion generally forms hydroxide complexes (e.g., UOH^{3+}, $U(OH)_4^0$). Under more oxidizing conditions, U^{+6} typically occurs as the uranyl ion (UO_2^{2+}), or the uranyl ion complexes with cations and anions that are common to abundant in groundwater, such as Ca^{2+}, Mg^{2+}, CO_3^{2-}, and HCO_3^-. Because of the formation of these soluble complexes, U^{+6} is typically more mobile than the other valence states over the pH and redox conditions common in many groundwater systems. Speciation modeling frequently shows the predominance of the $UO_2CO_3^0$, $(UO_2)CO_3(OH)_3^-$,

248 $Ca_2UO_2(CO_3)_3^0$, and $CaUO_2(CO_3)_3^{2-}$ species in groundwater (e.g., Dong and Brooks, 2006; Prat
249 et al., 2009; Zachara et al., 2013).
250
251 Fig. 2 shows the stability fields on an Eh-pH diagram of the minerals uraninite (UO_2),
252 schoepite ($UO_3 \cdot 2H_2O$), intermediate oxides (U_3O_8, U_3O_7, and U_4O_9), and various soluble species
253 when the total uranium activity in solution is fixed at 10^{-5} (~2.4 milligrams/liter [mg/L]). The
254 diagram shows a broad stability field for uraninite at low Eh (reducing conditions) across a wide
255 pH range. Also shown is the more restricted stability range in Eh-pH space of the intermediate
256 oxides. Note that the Eh-pH space occupied by these solids overlaps (near-neutral pH and
257 intermediate Eh) with many groundwater environments so that the intermediate oxides may be
258 important in controlling uranium concentrations in some groundwater systems (Langmuir, 1997).
259 At conditions representative of oxidizing environments, Fig. 2a shows a narrow field at near-
260 neutral pH controlled by schoepite. The Eh-pH diagram also indicates a wide range at low pH
261 and oxidizing conditions where the uranyl ion dominates and a wide region at alkaline pH and
262 oxidized/reduced conditions where uranyl-carbonate complexes dominate. Addition of dissolved
263 calcium to the system shows the influence of $Ca_2UO_2(CO_3)_3^0$ on uranium solubility; the presence
264 of this species enhances uranium transport potential by further corroding uraninite, schoepite,
265 and intermediate oxides at pH>7.
266
267 The solubility of the U^{+4} minerals including uraninite, pitchblende, and coffinite is extremely
268 low; consequently, the presence of reducing conditions effectively halts the movement of
269 uranium in groundwater. The ores contained in roll-front uranium deposits, for example,
270 typically consist of low-solubility uraninite and/or coffinite (e.g., Nash et al., 1981; Min et al.,
271 2005a). Therefore, research related to remediation of uranium-contaminated groundwater takes
272 advantage of sulfate-, iron-, and manganese-reducing bacteria to reduce uranium concentrations
273 to low levels by reductive processes (e.g., Lovley et al., 1991; Abdelouas et al., 2000; Yi et al.,
274 2007). Experimental work suggests that crystallinity, particle size, chemical impurity, and mixed
275 oxidation states all factor into uranium concentrations derived from uraninite dissolution (Finch
276 and Ewing, 1992; Langmuir, 1997; Casas et al., 1998). Fig. 2b shows the predicted solubility of
277 crystalline and amorphous uraninite based on thermodynamic data compiled in Langmuir (1997).
278 Note that the solubility of amorphous and crystalline uraninite is pH-independent above about

279 pH 4 to 4.5 and that the predicted solubility of crystalline uraninite from calorimetric
280 measurements is about nine orders of magnitude lower than the noncrystalline form (Langmuir,
281 1997). Such differences in solubility are also indicated in extraction studies that showed
282 noncrystalline forms of U^{+4} to be considerably more labile than uraninite (Cerrato et al., 2013).
283 The large differences in predicted solubility between experimentally-derived thermodynamic
284 data and calorimetric data deserve more examination.
285
286 Fig. 2c shows the predicted solubility of the U^{+6} minerals schoepite (β-$UO_3 \cdot 2H_2O$; data from
287 Jang et al., 2006) and soddyite ($(UO_2)_2(SiO_4) \cdot 2H_2O$; data from Gorman-Lewis et al., 2007) at
288 low and elevated values of PCO_2. Both minerals have v-shaped solubility trends with respect to
289 pH that differ from the solubility trends of U^{+4} minerals (see Fig. 2b). The solubility minima for
290 schoepite and soddyite occur over a restricted pH range at near-neutral pH; thus, these minerals
291 are least soluble at neutral pH and in low-CO_2 waters. The solubility minima for schoepite and
292 soddyite are below the EPA Maximum Contaminant Level (MCL) of 30 µg/L for uranium. With
293 increasing PCO_2 the solubilities of uranyl minerals increase, particularly at pH>8 due to the
294 stability of uranyl-carbonate complexes like $UO_2(CO_3)_3^{4-}$ and calcium-uranyl-carbonate
295 complexes. The solubility of soddyite depends on the aqueous concentration of silicon;
296 increasing silicon concentrations (i.e., to near cristobalite or amorphous silica saturation) will
297 decrease the equilibrium concentration of U^{+6}. In Fig. 2d, the role of phosphate in controlling U^{+6}
298 concentrations is illustrated. Precipitation of uranium with phosphate as autinite has the
299 possibility of achieving very low levels of residual uranium, particularly in low-CO_2 water.
300 Maximum solubility of uranium is seen in oxidizing, phosphate-free, carbonate-rich solutions;
301 these solutions are the principal reagents used for *in situ* leach mining of uranium in the US.
302
303 **3.1 Redox and the formation of roll-front deposits.**
304 The redox boundary where roll-front uranium deposits are formed is usually defined on the
305 basis of the geochemistry of its iron minerals, which occur in the oxidized state up-gradient of
306 the roll front and in the reduced state on the down-gradient side (Harshman and Adams, 1980).
307 However, details of the mineralogy and geochemistry of roll-front uranium ores can vary
308 significantly between deposits in a district and especially between deposits in different districts.
309 Here, a generalized description of roll-front deposits is presented, which is composited from

districts in the four states where ISR of uranium is ongoing (Texas, Wyoming, Nebraska, and South Dakota). It should be noted that roll-front deposits from China are generally similar to their US counterparts (Min et al., 2005a,b), which perhaps attests to the universal nature of redox processes forming the ores. A list of post-sediment-deposition minerals reported from the US ores is provided in Table 1. A transect from up-gradient to down-gradient through a roll-front uranium deposit illustrates the general mineralogy, geochemistry, and zonation of these ores (Fig. 3). Up-gradient of the roll front, the host sandstone has been oxidized by groundwater and iron is present as red hematite and perhaps magnetite, although both magnetite and Fe-Ti oxides in this zone may be completely oxidized (Goldhaber et al., 1978). An "alteration zone" commonly forms between the oxidized sandstone and ore in the roll front (Fig. 3) and this is generally interpreted to be the beginning of the oxidation of the ore zone as oxidized groundwater encroaches on it (Harshman and Adams, 1980). In this commonly yellow-colored zone, siderite and goethite typically occur, as does less abundant native sulfur and ferroselite, and detrital feldspars show alteration to clays in this zone (Rubin, 1970). The ore zone contains the uranium minerals uraninite, pitchblende, and coffinite; various iron sulfides; native selenium; clays; and calcite (Fig. 3). Kaolinite after detrital feldspar is ubiquitous in the ore zone (Rubin, 1970; Bowell et al., 2011); vanadium minerals may also occur (Fig. 4).

Reynolds and Goldhaber (1983) observed marcasite overgrowths on pre-ore pyrite and interpreted that phase to be an important ore-stage iron sulfide. Down-gradient from the uranium ore zone, molybdenum occurs as MoS_2 phases (Table 1) and arsenic apparently occurs in ore-stage iron sulfides. Arsenic, cobalt, and nickel are the most common trace elements found in low temperature pyrite (Huerta-Diaz and Morse, 1992; Saunders et al., 1997). The reduced or un-oxidized down-gradient sandstone typically contains pyrite and organic matter and exhibits a dark gray to green color (Galloway, 1978).

Metallic ore deposits that formed from aqueous solutions generally require at least four components working in conjunction to make a deposit (e.g., Barnes, 1997): (a) a source of metals; (b) a solution capable of transporting the metal(s); (c) a force driving solution flow; and (d) an effective precipitation mechanism. For sandstone-hosted roll-front uranium deposits, the source of uranium is typically uranium-rich source rocks such as granitic intrusive rocks or felsic

volcanic tuffs (Galloway, 1978; Nash et al., 1981). Models for roll-front uranium ore formation (e.g., Nash et al., 1981, Kyser and Cuney, 2008; Kyser, 2014) posit that uranium was leached from these rocks by oxidized meteoric water that subsequently infiltrated into shallowly dipping sandstone aquifers. Uranium is most soluble in oxidizing solutions containing bicarbonate, and both of these conditions apply to meteoric water in contact with the atmosphere (Langmuir, 1978). These oxidized uranium-bearing groundwaters flowed down-dip due to gravity-driven hydraulic gradients, until encountering a geochemical reducing agent. Reduction of U^{+6} to U^{+4} leads to precipitation of the highly insoluble (under reducing conditions) mineral uraninite (UO_2). Associated redox-sensitive elements such as V, As, Se, Mo, and Cr are also precipitated or sorbed in the redox-front and may be associated with iron sulfide minerals (Harshman and Adams, 1980). The principal reducing agent in the uranium roll-front systems is detrital organic matter (Nash et al., 1981; Kyser, 2014) but may also include iron sulfides or H_2S.

Southeast Texas roll-front uranium ores are virtually devoid of organic matter (Galloway, 1978) and apparently "sour gas" (methane + hydrogen sulfide) was the reductant. This sour gas is interpreted to have moved up faults into the ore-bearing formation from deeper hydrocarbon-bearing environments (Goldhaber et al., 1978; Reynolds et al., 1982; Reynolds and Goldhaber, 1983). Alternatively, Granger and Warren (1969) proposed that oxidation of iron sulfides could release metastable sulfur compounds such as thiosulfate ($S_2O_3^{2-}$) or polysulfides (S_n^{2-}) that could play important roles in redox reactions involved with roll-front ore formation. Rackley (1972; 1976) first proposed that bacteria played important roles in roll-front uranium ore formation. He proposed that aerobic bacteria facilitated mineral oxidation and dissolution up-gradient of the roll front, and anaerobic bacteria such as sulfate-reducers were important in precipitating reduced minerals in the roll-front ore zone. More recently, Min et al. (2005b) and Cai et al. (2007) described textures consistent with bacterial activity and preservation in uranium roll-front ores in northwestern China.

Many models (e.g., Granger and Warren, 1969; Harshman, 1972; 1974; Devoto, 1978; Harshman and Adams, 1980; Nash et al., 1981; Hobday and Galloway, 1999) for roll-front uranium deposit genesis include the concept that the roll fronts move down-dip in the host formation over time, as the redox boundary shifts due to the continuous incursion of oxidized

groundwater. However, recent research has shown that this interpretation might not be universally applicable, as at least one roll-front deposit (Three Crow in Nebraska) apparently has not moved appreciably. This interpretation is based on the lack of radiation-damage quartz textures up-gradient of the roll front (Leibold, 2013).

Although there has been about a 30-year hiatus on published detailed studies on the geology and geochemistry of US roll-front uranium deposits, there have been significant advances in related science areas that have implications for the genesis and post-mining remediation of such deposits. These advances include: (a) geomicrobiological controls on groundwater geochemistry in aquifers; (b) quantifying sorption of dissolved metal(loid)s on such minerals as Fe-Mn oxyhydroxides, clays, and sulfides; and (c) *in situ* bioremediation of metal(loid)-contaminated aquifers. Of those, the first perhaps has the most profound implications for roll-front uranium deposits. Numerous publications (e.g., Lovley and Phillips, 1988; Lovley, 1991; Chapelle and Lovley, 1992; Chapelle, 1993; Chapelle et al., 1995, Southam and Saunders, 2005; and U.S. EPA, 2007a,b) have demonstrated that bacteria in aquifers mediate (catalyze, speed up) geochemical reactions that are thermodynamically favored, which leads to a redox zonation in aquifers such as shown in Fig. 5.

As discussed above from the work of Langmuir (1978; 1997), uranium generally will form complex ions such as $UO_2CO_3^o$ in most natural groundwaters. Anaerobic Fe-reducing bacteria such as species of *Geobacter* have been shown to be able to reduce both ferric iron oxyhydroxide (e.g., goethite; Lovley, 1991) and the uranyl (U-VI) ion (Lovley et al., 1991; Anderson et al., 2003), and the following chemical reactions [1,2] illustrate this in terms of common roll-front mineralogy:

$$\text{FeOOH (goethite)} + \text{C (org.)} + UO_2CO_3^o + H_2O \xrightarrow{\text{(bacteria)}} Fe^{2+} + UO_2\ \text{(uraninite)} + 2HCO_3^- + \tfrac{1}{2}H_2 \quad (1)$$

or

$$\text{FeOOH (goethite)} + \text{C (org.)} + UO_2CO_3^o + H_2O \xrightarrow{\text{(bacteria)}}$$

403 $FeCO_3$ (siderite) + UO_2 (uraninite) + H_2CO_3 (aq) + ½H_2 (2)

404

405 These reactions would begin as shown in Fig. 4 upon encountering the Fe-reduction zone in an
406 aquifer and the redox conditions associated with it. Biogenic sulfate reduction can also cause
407 uranium precipitation (Lovley et al., 1993) if any is still dissolved by the time the sulfate-
408 reduction zone in the aquifer is encountered (Fig. 4). At the sulfate reduction zone, bacteria
409 mediate the reduction of dissolved sulfate to hydrogen sulfide:

410

411 (bacteria)

412 SO_4^{2-} + 2C (organic) + $2H_2O$ = H_2S (aq) + $2HCO_3^-$ (3)

413

414 and then the H_2S reacts with any available ferrous iron to make an iron monosulfide:

415

416 Fe^{2+} + H_2S (aq) = FeS (mackinawite) + $2H^+$ (4)

417

418 which eventually leads to formation of the thermodynamically favored iron disulfide, pyrite
419 (Rickard and Luther, 1997) or perhaps marcasite if pH is low enough (<~6, Reynolds and
420 Goldhaber, 1983; Murowchick and Barnes, 1986). Thus, the bacteria mediate the geochemical
421 reactions that lead to uranium mineral precipitation and changes in iron mineralogy. However,
422 these bacterially mediated geochemical processes involving organic carbon, iron, and sulfur are
423 typical of most anaerobic confined aquifers (e.g., Chapelle, 1993), irrespective of whether minor
424 amounts of uranium are present in solution. Apart from establishing redox conditions in
425 groundwater, the direct role that microbes may or may not play in the formation of roll-front U
426 deposits is an area of continuing research.

427

428 Sorption of uranium and associated metals and metalloids on mineral surfaces in groundwater
429 systems has been proposed to be an important process in uranium roll-front formation (e.g., Nash
430 et al., 1981; Cuney, 2010). Uranium and associated metals and metalloids (As, Se, V, Mo) in the
431 roll-front ores all apparently have the capability of being sorbed by four common classes of high-
432 surface-area minerals in the roll-front systems: (a) clays (Ames et al., 1983; Wang et al., 2011);
433 (b) iron oxyhydroxides (Dzombak and Morel, 1990); (c) manganese oxyhydroxides (Tani et al.,

2004; Wang et al., 2012; and Mukherjee et al., 2013), and (d) sulfide minerals (Saunders et al., 1997; Lee and Saunders, 2003; Southam and Saunders, 2005; Scott et al., 2007; Descostes et al., 2010). The stability of these mineral phases is a function of both changing redox geochemistry and diagenetic reactions, and thus is likely complex and evolves over time. Similarly, sorption reactions for uranium and associated elements in the roll-front ores need to be considered in planning for effective aquifer restoration technologies.

In situ bioremediation processes have been demonstrated in the field for metal(loid)-contaminated groundwater (including uranium) using both iron-reducing bacteria (e.g., Anderson et al., 2003) and sulfate-reducing bacteria (Saunders et al., 2005; 2008; Tang et al., 2013; Watson et al., 2013; Wu et al., 2006). Taken together, these approaches are apparently analogous in real time to the important redox geochemical and geomicrobiologic processes that were involved in the formation of roll-front uranium ores. The bioremediation time period corresponds to the aquifer changing from oxidized aerobic conditions, progressing through Fe-reduction, and reaching sulfate-reducing conditions (Saunders et al., 2005). A field demonstration project (Saunders et al., 2005; 2008) designed to remove metals that form sulfide minerals (Cu, Pb, Cd) illustrated the geochemical behavior of redox sensitive elements U, Cr, and Se in the process, and thus, *in situ* bioremediation projects can provide insights into uranium roll-front ore-forming processes. Further, such *in situ* bioremediation approaches are showing considerable promise in remediating aquifers after ISR operations (Long et al., 2008; Hall, 2009).

4. Hydrogeologic Characteristics of Roll Front Deposits and Related Aquifer Systems and Adjacent Confining Units

Roll-front deposits are contained in dipping sandstone bodies confined above and below by less permeable shale or mudstone. Groundwater recharge areas generally occur up-gradient and up-dip of the uranium ore body, and lead to groundwater down-gradient migration through the ore body. In numerous publications on uranium roll-front deposits and ISR, hydrogeologic characterization of the aquifer systems related to the ore body host rock and adjacent confining units is often not discussed (or is minimally discussed). However, as part of the permitting and licensing process for uranium ISR sites, a significant amount of site-specific hydrogeologic information may be expected to be collected. During the initial licensing review, a generalized

466 characterization of the site is expected in order to have an understanding of the natural system;
467 after licensing, this is followed by more extensive characterization including hydrogeologic
468 characterization (e.g., conducting pump tests to collect information on aquifer properties) (NRC,
469 2009a). A licensing review is conducted by the U.S. Nuclear Regulatory Commission (NRC) and
470 includes a significant amount of hydrologic and hydrogeologic information in order to "*establish*
471 *potential effects of in situ leach operations on the adjacent surface-water and ground-water*
472 *resources*" (NRC, 2003). The required information includes: i) description of surface-water
473 features in the site area; ii) assessment of the potential for erosion or flooding; iii) a description
474 of site hydrogeology; iv) assessment of available groundwater resources and groundwater quality
475 within the proposed permit boundaries and adjacent properties; v) an assessment of typical
476 seasonal ranges and averages and the historical extremes for levels of surface-water bodies and
477 aquifers; and vi) information on past, current, and anticipated future water use, including
478 descriptions of local groundwater well locations, type of use, amounts used, and screened
479 intervals.
480
481 The site hydrogeology description includes: (a) identification of aquifer and aquitard
482 formations that may affect or be affected by the *in situ* leach operations; (b) description of
483 aquifer properties, including material type, formation thickness, effective porosity, hydraulic
484 conductivity, and hydraulic gradient; (c) estimated thickness and lateral extent of aquitards, and
485 other information relative to the control and prevention of excursions; and (d) data to support
486 conclusions concerning the local groundwater flow system, based on well borings, core samples,
487 water-level measurements, pumping tests, laboratory tests, soil surveys, and other methods.
488
489 Groundwater monitoring wells are an integral part of the ISR operation; however, these wells
490 are primarily installed to monitor for potential excursions of the leaching solution from the ISR
491 area. The NRC (2009b) provides general information on monitoring well placement, and
492 indicates that specific requirements are site-specific. The placement of the ISR monitoring wells
493 around the well fields and in the aquifers above and below the well field is "*based on what is*
494 *known about the nature and extent of the confining layer and presence of drill holes, hydraulic*
495 *gradient, and aquifer transmissivity and well abandonment procedures used in the region. For*
496 *example, monitoring wells should be placed downgradient from the production zone to detect*

excursion plumes. Monitoring wells completed in the uranium bearing horizon must be in hydraulic communication with the production zone to be effective (i.e., groundwater can easily flow between the production zone and the monitoring wells). Additional, more closely spaced wells may be necessary if there are preferred flow paths in the aquifer" (NRC, 2009b).

5. Lixiviants, the Leaching Solutions

The leaching fluid in the ISR mining process is referred to as the lixiviant solution. Lixiviant solutions are injected into the ore zone and the mixed leaching fluid and groundwater are then pumped out of the ground at a production well. The ideal lixiviant is one that will both oxidize the uranium in the ore and also contains a complexing agent. The latter will aid uranium dissolution and form strong aqueous complexes that remain dissolved and interact little with the host rocks (Davis and Curtis, 2007). Two general approaches have and are being used for the *in situ* mining of uranium internationally, which are a function of the increased solubility of uranium oxide at both low and high pH conditions (Mudd, 2001; see Fig. 2). Acid leaching, which is predominantly used in former Soviet republics and Australia, involves the injection of a relatively dilute solution of a strong acid (typically sulfuric or hydrochloric). This technique is most effective if carbonates or other acid-neutralizing minerals are present as minor constituents in the ore zones and adjacent areas. Carbonate-rich ores require proportionally more acid for equivalent uranium recovery and carbonate dissolution promotes gypsum precipitation that leads to porosity reduction in the ore zone and less efficient uranium recovery (Ben Simon et al., 2014).

In addition, acid leaching has the added disadvantage of dissolving associated heavy metals and metalloids, particularly if they are bound up in sulfide minerals or sorbed onto mineral surfaces such as goethite (e.g., Dzombak and Morel, 1990). In the US, although acid leaching has been used in the past (Mudd, 2001), today alkaline leaching is used exclusively due to high calcite contents of ores and also environmental concerns about releases of heavy metals and metalloids to groundwater. Early (1970s to 1980s) *in situ* leaching of uranium involved using air, sodium chlorate, sodium hypochlorite, or potassium permanganate as oxidants, which were often mixed with sodium or ammonium carbonate-bicarbonate to enhance uranium solubility by forming aqueous U-CO_3 complexes (Deutsch et al, 1984; Rojas, 1989; Davis and Curtis, 2007). Up until about 1981, virtually all of these sites utilized alkaline reagents such as ammonia- or

sodium-carbonate/bicarbonate. The difficulty of restoring ammonia-based sites led to a quick shift in emphasis to sodium bicarbonate- or carbon dioxide-based leaching chemistry by the early 1980s (Anastasi and Williams, 1984; Mudd, 2001). State-of-the-practice today in the US involves using O_2 and CO_2 gas in the initial injection solution (Campbell et al., 2007; NRC, 2009a,b; Johnson et al., 2010), which also accomplishes the oxidation and aqueous-complexing requirements to enhance uranium dissolution. Chemical reactions illustrating the uranium oxidative dissolution (by molecular oxygen or hydrogen peroxide) and complexing are shown below:

Oxidation:

$$UO_2 \text{ (uraninite)} + \tfrac{1}{2}O_2 + 2H^+ = UO_2^{2+} \text{ (uranyl)} + H_2O \quad (6)$$

Or, if hydrogen peroxide is the oxidizing agent

$$UO_2 \text{ (uraninite)} + H_2O_2 + 2H^+ = UO_2^{2+} \text{ (uranyl)} + 2H_2O \quad (7)$$

Complexation:

$$UO_2^{2+} + 2Ca^{2+} + 3HCO_3^- = Ca_2(UO_2)(CO_3)_3^o + 3H^+ \quad (8)$$

This approach can be augmented by subsequent addition of stronger reagents on a case-by-case basis (Susan Brown, USGS, personal communication, 2014). Increasing pH>~8 can liberate Se and As oxyanions sorbed onto iron-oxyhydroxides (Smedley and Kinniburgh, 2002; Goldberg, 2014), and this can be a trigger to mobilize these anions and impact down-gradient water resources in situations where natural attenuation processes are insufficient to sequester these arsenic and selenium anions. Table 2 provides groundwater quality data for selected metals prior to ISR and after aquifer restoration at several sites in Wyoming and Nebraska (Anastasi and Williams, 1984; Davis and Curtis, 2007; Borch et al., 2012). The water quality data indicate that several trace metals and anions including As, Se, Mo, V, Mn, Fe, U, Ra, and sulfate are likely to be liberated during ISR and may remain in groundwater even after post-ISR restoration efforts

560 are completed. Once established, groundwater uranium plumes can be persistent due to slow
561 desorption of uranium from aquifer solids and slow oxidative dissolution of reduced uranium
562 (Zachara et al., 2013). This suite of potential trace metal contaminants is likely to be site-specific
563 and depend on factors such as the ore geology, ore and gangue composition, and nature of ISR
564 operations. For example, the presence of clay minerals in the ore zones can sorb uranyl species
565 and thus there is a degree of ''preg-robbing'' by some clay minerals in uranium ores (Bowell et
566 al., 2011). Post-mining aquifer restoration can also be complicated by the fact that leaching is not
567 100% efficient, and some lixiviant is left behind in the ore zone (Stover, 2004).
568
569 **6. Observation and Extraction Well Design and Placement**
570
571 **6.1 Observation wells for monitoring groundwater during the ISR operations.**
572
573 ISR can be accomplished by allowing natural groundwater flow to move injected solution
574 (lixiviant) toward extraction wells, but more commonly, active pumping of extraction wells is
575 utilized because regional groundwater flow is generally slow (less than 50 feet per year; [Way,
576 2008]). In order to ensure containment, the total pumping rate is generally 1 to 3 percent higher
577 than the total injection rate. The idea is to create an inward flow gradient and to control lixiviant
578 flow (Way, 2008). Geometric patterns of injection and extraction wells are typically utilized,
579 where injection wells are generally located on the outside of the pattern and extraction wells in
580 the interior (Deutsch et al., 1984; U.S. EPA, 1995; Mudd, 2001; Campbell et al., 2007). In the
581 US, production life of an individual ISR well pattern is typically one to three years and most
582 uranium is recovered during the first six months of the operation. Typical uranium extraction
583 efficiencies range from 60 to 80% (World Nuclear Association, 2014). Maintaining adequate
584 lixiviant flow rates into the ore formation is often difficult in ISR operations due to aquifer
585 plugging. This can be caused by microbe growth and swelling-dispersion of clays (Pugliese and
586 Larson, 1989), by suspended particles entrained in the injection solution (Pastukhov et al., 2014),
587 or by precipitation of iron oxyhydroxides.
588
589 A variety of well-field configurations have been proposed or used, such as regular four-spot,
590 skewed four-spot, five-spot, seven-spot, inverted seven-spot, nine-spot, inverted nine-spot, direct
591 line drive, or staggered line drive (Ward, 1983; Osiensky and Williams, 1990). After uranium

ISR is completed, the well field can be used for restoration of the groundwater at the ISR site. These wells provide monitoring points to assess the status of the restoration.

Site-related observation wells are an integral part of ISR operations, to monitor for excursions (releases) of the lixiviant from the ISR area into surrounding areas. The placement of these wells is based on an understanding of the hydrogeologic properties and knowledge of the extent of the uranium-bearing portions of the aquifer. In addition, some of these wells are to be located in aquifers above and below the uranium-bearing aquifer, as well as outside the ISR or exempt area. The number, locations, areal density, depths, and screen placement are likely to be site-specific, and specified in licensing (e.g., NRC, 2009b) and operating documents. For example, monitoring wells are located about 150 m (500 ft) beyond the well field and with a maximum separation of 150 m (500 ft) at the Smith Ranch ISR, WY, and were proposed to be located 140 m (460 ft) beyond the outermost production and injection wells (and with a maximum separation of 140 m [460 ft]) at the proposed Crownpoint, NM ISR site, to monitor for horizontal excursion of lixiviant (NRC, 2009b).

Spacing of monitoring wells in overlying and underlying aquifers is also site-specific and variable, with ranges from 1 well per 1.2 ha (3 acres) to 1 well per 2 ha (5 acres). In some cases, the underlying confining layer may be very thick and the underlying aquifer not used as a source of water, so the underlying aquifer may not need to be monitored (such as at the Crow Butte ISR site, Nebraska, where the underlying confining layer is more than 300 m [1,000 ft] thick and the underlying aquifer is not used) (NRC, 2009b). However, it is important to establish through geologic and hydrologic evaluations that stratigraphic units presumed to be confining layers are in fact impermeable to contaminant migration.

As part of the ISR license application, the site characterization requires the applicant to survey and report locations of all privately owned wells within 3.3 km (2 mi) of the permit area and their current uses and production rates to assess potential impacts on these wells due to the ISR operations. Routine monitoring of all down-gradient wells that could be used for drinking water, livestock watering, or crop irrigation is also required (NRC, 2009b).

6.2 Additional wells for monitoring post-ISR groundwater

Development of a post-ISR monitoring well program for down-gradient (and side-gradient) groundwater can use the hydrogeologic characterization information obtained during the licensing and development process. However, additional hydrogeologic characterization may be needed if the focus is on the quality of groundwater migrating further down-gradient than the boundary of the lixiviant-excursion-based ISR groundwater monitoring program. The geologic and hydrogeologic conditions may vary further down-gradient, and groundwater supply wells may be screened in different units or aquifers than the uranium-bearing aquifer.

Planning a monitoring well system for the groundwater down-gradient of an existing or former ISR site takes into consideration a number of factors that cover the dynamic changes that will occur in the restoration and post-restoration phases as the aquifer returns to pre-mining conditions, including:

1. The need for a three-dimensional (3D) conceptual site model (CSM), due to subsurface heterogeneity and spatial variability. A 3D CSM may be especially important for monitoring groundwater in roll-front deposits and in down-gradient regions, due to often numerous interbedding of layers having different permeabilities and hydraulic conductivities.
2. Location of down-gradient receptors (e.g., groundwater supply wells, surface water). This includes the elevation and hydrostratigraphic position of the groundwater supply well screens or open borehole.
3. Piezometric surface elevation and changes in the elevation.
4. Direction (and changes in direction) of groundwater flow.
5. Velocity of groundwater and potential contaminants. This is determined through knowledge of the hydraulic conductivity and gradient, porosity, effective porosity, and contaminant fate and transport processes. The velocity can be used to site wells at a distance representing a given groundwater and contaminant travel time.
6. Vertical leakage/migration of groundwater via boreholes, fracture, faults, and/or leaky confining layers.
7. Groundwater extraction rate in down-gradient water supply wells. This affects the extent of the capture zone for the well.

8. Degree of penetration of the screen into a particular hydrostratigraphic unit. This can influence the flow path of groundwater to the screen while pumping.
9. Length of the screen or open borehole. This can impact any water quality measurements, due to the possibility of dilution of contaminated groundwater with cleaner groundwater.

A conceptual monitoring network that may be applied to a variety of contaminant plumes is provided in Fig. 6 (from Pope et al., 2004). It shows the target monitoring zones necessary to assess a contaminant plume: up-gradient and side-gradient (background), source zone (the ISR exempted aquifer area), high concentration plume core, low concentration plume fringes, plume boundaries, and down-gradient regions. It also indicates the use of transects across a plume, which can be used to better understand the configuration of the plume and the contaminant flux. Such a network may be used if a uranium (or other constituent) plume has migrated down-gradient of the ISR site.

6.3 Modeling aspects of site monitoring

Both analytical and numerical models may be used to predict groundwater flow and contaminant transport to support the design of monitoring well networks. Analytical models are not generally appropriate for modeling the complex flow and transport patterns that occur under the influence of uranium ISR injection/extraction schemes, and thus are not well-suited to the design of monitoring well networks for active uranium ISR operations. Depending upon the system hydrogeology and the time required to return to a near steady-state flow condition following the cessation of ISR, analytical models can potentially be used to support the design of monitoring well networks installed post-ISR.

Numerical models are generally much more flexible and powerful than analytical models. They can be readily used to support the design of monitoring well networks by: i) predicting flow patterns during and after uranium ISR; ii) performing groundwater particle tracking to assess flow paths; and iii) simulating contaminant transport. Among available numerical modeling codes, the MODFLOW (Harbaugh, 2005) family of finite-difference codes (e.g., MODFLOW, MODPATH [Pollock, 1994], MT3DMS [Zheng, 2010], etc.) is typically the default choice for simulating groundwater flow and contaminant transport, given that this

program: has the ability to simulate a broad range of hydrogeologic conditions; is a proven open-source, well-documented, public-domain code; has acceptance by regulatory agencies; and is supported by various public-domain and proprietary graphical user interfaces. MODFLOW may not be the most appropriate code for simulating certain conditions in support of the design of monitoring well networks. Such conditions include local aquifer dewatering, complex aquifer geometry, and secondary porosity (e.g., faults, fractures, conduits). Dewatering may occur in modeling of uranium ISR due to simulation of groundwater extraction, which often causes instability in MODFLOW. Alternate codes in this case include:

1. MODFLOW-NWT (public-domain) (Niswonger, 2011) and MODFLOW-SURFACT (proprietary) (HydroGeoLogic, 1996): Finite-difference codes with public-domain and proprietary graphical user interfaces.
2. FEFLOW (DHI-WASY, 2013): Proprietary, finite-element code integrated with a graphical user interface.
3. FEHM (Zyvoloski, 2007): Public-domain, finite-element code without a graphical user interface.

Alternatives to MODFLOW in cases where simulation of complex aquifer geometry and secondary porosity are important include MODFLOW-USG (a recent finite-volume extension of MODFLOW) (Panday, 2013) and finite element codes such as FEFLOW and FEHM. In general, simulation of secondary porosity is unlikely to be required for uranium ISR sites, given that most are in sandstone settings, where secondary porosity is typically not significant.

Once constructed, numerical models can be used to simulate groundwater flow patterns, flow paths, and contaminant transport in order to design appropriate monitoring well networks. In addition, numerical optimization approaches may be used to assist in defining optimal monitoring well locations. Multiple (typically hundreds to thousands of) model realizations may be developed and simulated, varying key model parameters affecting contaminant transport (e.g., hydraulic conductivity, sorption, etc.). These multiple realizations may then be evaluated together using statistical methods to assess the most likely transport pathways and the optimal distribution of monitoring points.

If contaminants are detected in the monitoring well network, numerical models may be used to simulate containment and recovery approaches. Location and rates for extraction wells may be optimized using codes such as MODOFC (Ahlfeld and Riefler, 1996) and GWM-2005 (Ahlfeld et al., 2009), which work in concert with MODFLOW to define optimal pumping networks (e.g., minimum number of wells and minimum pumping rates) for achieving a defined objective.

Models used to simulate reactive transport typically incorporate rate-limited geochemical reactions, mineral dissolution and precipitation, adsorption/desorption at the mineral-water interface, and consequent changes in porosity and permeability as a result of these reactions. Reactive transport models can be used to help constrain water quality impacts from chemical injections (e.g., Ben Simon et al., 2014). For contaminant transport, a simple equilibrium-sorption approach may be assumed to describe the partitioning of contaminants between the solid and the liquid phases. Codes like MT3DMS, MODFLOW-SURFACT, RT3D (Clement, 2002) and HYDROBIOGEOCHEM123 (Gwo et al., 2001) (both MODFLOW-linked), PHAST (Parkhurst et al., 2010), and TOUGH series codes (Xu et al., 2006) may be used. Parameters related to geochemical rates are generally lacking, particularly kinetic data on mineral-water reactions involving metals and metalloids. Petrographic, mineralogical, and geochemical studies of core samples from ISR sites are needed to feed into the model architecture (see WoldeGabriel et al., 2014 and Gallegos et al., 2015).

7. Impact of Off-Site, Adjacent Water Wells on Groundwater Flow and Potential Solute Fate and Transport

Off-site or adjacent groundwater supply wells (private, municipal, irrigation, etc.) may be impacted by any contaminants in the ISR area that have migrated down-gradient. It is possible that some wells may be in a direct down-gradient contaminant migration pathway; however, it is more likely that a pumping well (especially at high pumping rates) may be impacted by the plume and/or have an impact on the direction of the plume. A pumping well will have an up-gradient capture zone of horizontal and vertical extents that depend on the rate of pumping, the hydrostratigraphic unit that the well is located in, the screen or open borehole position and length, the hydraulic conductivity, the hydraulic gradient, porosity, and the saturated thickness.

Estimation of the capture zone of wells in the vicinity of the ISR site is important in evaluating the potential for contamination of the groundwater supply well. It is not only the groundwater supply wells in the general down-gradient direction of the ISR site that may need to be evaluated, but wells that are side-gradient, as a high pumping rate may lead to a wide capture zone that extends laterally toward the ISR site. A thorough discussion of evaluating capture zones is provided in U.S. EPA (2008).

In order to evaluate the impacts of nearby, off-site water supply wells upon groundwater flow patterns and contaminant transport at uranium ISR sites, the modeling considerations are generally similar to those discussed in the preceding section. Such off-site water supply wells may be incorporated into models to predict (a) whether contaminants may be drawn toward the wells; (b) where monitoring wells should be located to detect such migration; and (c) how the uranium ISR system may be best modified to avoid potential negative impacts to water supply wells.

If a site-specific numerical model is not available, simple larger-scale models can be constructed as a screening-level tool to assess whether uranium ISR operations may impact a nearby water supply well. These simple models may make use of available regional information on hydraulic gradient and conductivity to assess whether a production well is close enough and/or operating at a high enough rate to interact significantly with the uranium ISR operation. If this simple screening model suggests the potential for significant interaction, a site-specific numerical model may then be constructed to better evaluate the potential for negative interactions.

8. Identification of Potential Aquifer Vulnerabilities to *In Situ* Recovery Operations

Previous sections in this review identified many hydrogeologic factors, some of which may influence the potential for contamination of an aquifer due to ISR operations. Two negative scenarios are excursion of lixiviant during ISR and down-gradient migration of uranium ISR-related contaminants after ISR operations are completed (e.g., trace metals, metalloids, sulfate). An aquifer may be vulnerable to these scenarios in a number of ways:

1. The presence of faults that are either undetected or mis-characterized may lead to contaminant migration along the faults (either horizontally or vertically).

2. The presence of numerous sandstone, siltstone, and mudstone (as well as their unconsolidated forms, and clay) interbeds at some roll-front locations can influence the distribution of lixiviant as well as uranium- and ISR-related contaminants. If such interbeds extend in directions or distances that are not well understood, contamination may extend beyond the ISR well field.

3. Undetected preferential flow paths can lead to contaminant migration in unexpected directions or poorly quantified groundwater or contaminant flux. The fluvial sedimentary environment in some roll-front deposits may result in preferential flow paths in more permeable sandstone lenses.

4. The numerous boreholes in an ISR well field may include some that are not completely grouted or cased, and which may allow vertical flow along a borehole into overlying or underlying permeable units.

5. The presence of nearby groundwater supply pumping wells may lead to capture zones that intersect the exempt ISR area or areas having down-gradient migration of ISR-related contaminants.

6. Unreacted ore material may serve as a continuing source of contaminants to groundwater after ISR is complete.

9. Data Gaps, Appropriate Monitoring Strategies, Key Elements for Modeling Applications, and Post-ISR Aquifer Restoration

9.1 Data gaps

Data gaps may include:

1. Poorly understood stratigraphy due to insufficient logging of subsurface materials and wells/boreholes (e.g., the lack of geophysical methods).

2. Undetected preferential flow paths that may be due to short-circuiting along poorly sealed wells/boreholes, the fluvial depositional environment of the aquifers, or unidentified or poorly characterized faults.

3. Insufficient capture zone analysis of nearby wells. U.S. EPA (2014) indicates a quarter mile "buffer zone" at the Goliad, TX proposed ISR site in which any wells were evaluated for capture zones; however, the extent of a necessary "buffer zone" may vary from site to site. Groundwater

velocities, the estimated travel times from an ISR site to a nearby well, and the rate of pumping of the well could conceivably impact the distance through which capture zones may need to be evaluated.

4. Poorly understood geochemistry in the areas down-gradient of an ISR site. Since the subsurface geochemistry strongly impacts the fate and transport of the ISR-related contaminants, lack of knowledge regarding the geochemistry, solid phase and groundwater, may lead to poorly estimated contaminant travel times.

9.2 Appropriate monitoring strategies

An appropriate monitoring strategy depends on an adequate understanding of the stratigraphy (depositional environment) and structural geology (e.g., faults); groundwater flow direction and its possible temporal changes; hydraulic conductivity and hydraulic gradient (to estimate groundwater flow velocities); and locations, pumping rates, and pumping patterns of nearby groundwater supply wells. Based on these site-specific factors, the locations for monitoring wells down-gradient and side-gradient from the ISR site, and the spacing of these wells, can be determined. It appears obvious that monitoring wells be located up-gradient of any groundwater supply wells in the vicinity of the ISR site. Such monitoring wells may be located a given distance from the groundwater supply well (the distance to be calculated using estimates of the groundwater velocity and a desired "warning" period of time between the monitoring well and the groundwater supply well).

Conceptually, a monitoring strategy could include: i) installation of monitoring wells a specific distance down-gradient of the boundary of the ISR site; ii) installation of monitoring wells in aquifers above and below the uranium roll-front deposit/ISR zone; iii) multi-level or nested monitoring wells, with screens or open borehole lengths placed in zones of higher permeability and greater groundwater flow; iv) evaluation of the capture zones of nearby groundwater supply pumping wells, and installation of up-gradient wells outside the boundary of the capture zone, as well as within it; and v) proper sampling and analytical techniques for the potential contaminants related to uranium ISR sites, to ensure that the contaminants and geochemical parameters are representative of the aquifer.

9.3 Key elements for modeling applications

Based on the discussion in previous sections, key elements for modeling may include: i) an understanding of the stratigraphy and properties of the various units encountered (and representing these properly in inputs to the model); ii) the subsurface geochemistry (groundwater and aquifer solids) and contaminant concentrations, and the parameters that impact the fate and transport of the contaminants; and iii) the groundwater velocities and fluxes in the hydrogeologic units that contribute the greatest contaminant flux for down-gradient migration.

9.4 Post-ISR aquifer restoration

After ISR mining operations have ceased, mining companies are required to restore groundwater quality to pre-mining concentrations for metals, metalloids, anions, and total dissolved solids. Several approaches have been used to restore groundwater quality, including groundwater sweeping, reverse osmosis treatment, subsurface injection of chemical reductants, bioremediation, and monitored natural attenuation (MNA) (e.g., Borch et al., 2012; Gallegos et al., 2015). Groundwater sweep restoration involves pumping one or more pore volumes from the targeted mining zone followed by treatment or disposal of the extracted water. Uncontaminated regional groundwater is then expected to flow into the zone of displaced groundwater. Next, reverse osmosis restoration involves continued groundwater extraction, treatment, and re-injection of the treated water into the subsurface. In-situ chemical reduction and bioremediation technologies make use of chemical amendments to drive immobilization of redox-sensitive elements; such remediation processes have been demonstrated in the field for metal(loid)-contaminated groundwater (including uranium) using iron-reducing bacteria (e.g., Anderson et al., 2003), sulfate-reducing bacteria (e.g., Saunders et al., 2005; 2008; Wu et al., 2006; Watson et al., 2013), and injections of reductants such as dithionite, ferrous iron, or sulfide (e.g., Ludwig et al., 2007). The U.S. EPA has developed a series of technical framework documents that should be consulted for the application of MNA as a tool to restore aquifers following ISR operations (US EPA, 2007a; 2007b; 2010). The approach is a four-tiered assessment of MNA as a viable response action for selected metal, metalloid, and radionuclide contaminants encountered in groundwater and involves the following: i) demonstrating contaminant sequestration mechanisms; ii) estimating attenuation rates; iii) estimating attenuation capacity of aquifer solids; and iv) evaluating potential reversibility issues. Overall, MNA is likely to be more

879 applicable as a polishing step and/or under more dilute plume concentrations as compared to
880 situations encountered in source zones or in more concentrated regions of a groundwater plume
881 (Ford et al., 2008).
882
883 Borch et al. (2012) concluded that groundwater sweeping followed by reverse osmosis
884 treatment was highly efficient. However, subsequent injection of a reductant in the form of
885 dissolved H_2S did not further reduce concentrations of U, Mn, or Fe. WoldeGabriel et al. (2014)
886 suggested that pyrite surfaces that are accessible to migrating groundwater could act as
887 reductants to limit the migration of U; consequently, solid-phase aquifer characterization studies
888 are critical in examining the potential for natural attenuation (see US EPA, 2007a). In addition,
889 recent work by Basu et al. (2015) indicates that isotopic tracers such as $^{238}U/^{235}U$ ($\delta^{238}U$) and
890 $^{34}S/^{32}S$ ($\delta^{34}S$) may be used to trace ore zone groundwater after mining has ended as a probe of
891 natural attenuation processes (see also Brown et al., 2016). A range of geochemical pathways
892 have been studied that show promise for transforming uranium to less mobile forms, including
893 co-precipitation with iron oxides (e.g., Duff et al., 2002; Nico et al., 2009; Marshall et al., 2014),
894 co-precipitation with phosphate (e.g., Mehta et al., 2015), and reduction by iron- or sulfur-
895 containing minerals (e.g., Moyes et al., 2000; Scott et al., 2005; Hyun et al., 2012; Troyer et al.,
896 2014).
897
898 **10. Conclusions**
899
900 Environmental concerns during and after ISR include potential migration of leaching solutions
901 away from the injection zone into down-dip, underlying, or overlying aquifers. Uranium, its
902 decay products, and a number of redox-sensitive trace metals (e.g., Fe, Mn, Mo, Se, V),
903 metalloids (As), and anions (sulfate) of environmental concern may migrate in the groundwater.
904
905 Monitoring wells are located up- and down-gradient of the production area to determine if
906 contaminant migration occurs. Monitoring strategies could include installation of monitoring
907 wells down-gradient of the boundary of the ISR site; installation of monitoring wells in aquifers
908 above and below the ore body and ISR zone; multi-level or nested monitoring wells; capture
909 zone evaluation of nearby groundwater supply pumping wells; and installation of up-gradient

wells outside the boundary of the capture zone, as well as within it; and proper sampling techniques for the potential contaminants related to uranium ISR sites, to ensure that the contaminants and geochemical parameters are representative of the aquifer.

Potential aquifer vulnerabilities to *in situ* recovery operations include undetected or mis-characterized faults that may result in contaminant migration along the faults; the presence of numerous sandstone, siltstone, and mudstone lenses that can influence the distribution of lixiviant as well as uranium- and ISR-related contaminants; undetected preferential flow paths that could lead to contaminant migration in unexpected directions; the numerous boreholes in an ISR well field that may allow vertical flow along a borehole into overlying or underlying permeable units; and the presence of nearby groundwater supply pumping wells that may lead to capture zones that intersect the exempt ISR area or areas having down-gradient migration of ISR-related contaminants. Data gaps in an existing conceptual site model may include any of these potential vulnerabilities. Poorly understood geochemistry in the areas down-gradient of an ISR site may lead to inaccurate estimates of contaminant concentrations and velocities.

Research related to remediation of uranium-contaminated groundwater takes advantage of biotic (sulfate-reducing bacteria) and abiotic processes (reductive precipitation and co-precipitation) to reduce uranium concentrations to low levels, and the literature indicates that *in situ* remediation has been successfully demonstrated in the field in some cases for metal(loid)-contaminated groundwater (including uranium) using both biotic and abiotic pathways. MNA assessments should include: i) demonstration of contaminant sequestration mechanisms; ii) estimates of attenuation rates; iii) estimates of the attenuation capacity of aquifer solids; and, iv) evaluation of potential reversibility issues.

Suggestions for future work to better understand the subsurface geochemistry related to uranium roll-front deposits, and to develop effective post-ISR monitoring programs, include:

- Conducting modern multi-element analyses of samples from traverses through roll-front ores using ICP-OES and ICP-MS techniques, microscopy, and new detailed spectroscopic studies of aquifer minerals and their trace metal associations. This will

allow for an improved understanding of potential contaminant mobilization and attenuation processes.

- Drilling of cores post-leaching and post-aquifer restoration for comparison to pre-mining cores to better understand leach-ore-gangue mineral reactions, particularly reactions involving groundwater and potential contaminants of concern.

- Evaluation of *in situ* remediation techniques to improve post-mining aquifer restoration efforts.

Acknowledgements

The U.S. Environmental Protection Agency through its Office of Research and Development funded the research described here. It has not been subjected to agency review and therefore does not necessarily reflect the views of the agency, and no official endorsement should be inferred. Mention of trade names or commercial products does not constitute endorsement or recommendation for use. We thank Dave Burden and Dan Pope for their help with this project. The manuscript was improved by comments of three anonymous reviewers.

References

Abdelouas, A., Lutze, W., Gong, W., Nuttall, E.H., Strietelmeier, B.A., Travis, B.J., 2000. Biological reduction of uranium in groundwater and subsurface soil. Sci. Total. Environ. 250, 21-35.

Ahlfeld, D.P., Riefler, R.G., 1996. Documentation for MODOFC: A program for solving optimal flow control problems based on MODFLOW simulation, Report RCGRD#96-20, University of Connecticut, Storrs, CT.

Ahlfeld, D.P., Baker, K.M., Barlow, P.M., 2009. GWM-2005 - A groundwater-management process for MODFLOW-2005 with local grid refinement (LGR) capability. U.S. Geological Survey Techniques and Methods 6-A33.

Ames, L.L., McGraph, J.E., Walker, B.A., 1983. Sorption of trace constituents from aqueous solutions onto secondary minerals. I. Uranium. Clays Clay Min. 31, 321-334.

Anastasi, F.S., Williams, R.E., 1984. Aquifer restoration at uranium *in situ* leach sites. Internat. J. Mine Water 3, 39-37.

Anderson, R.T., Vrionis, H.A., Ortiz-Bernad, I., Resch, C.T., Long, P.E., Dayvault, R., Karp, K., Marutzky, S., Metzler, D.R., Peacock, A., White, D.C., Lowe, M., Lovley, D.L., 2003. Stimulating the *in situ* activity of Geobacter species to remove uranium from the groundwater of a uranium-contaminated aquifer. Applied Environ. Microbiol. 69, 5884–5891.

Barnes, H.L., 1997. Geochemistry of Hydrothermal Ore Deposits (3rd ed.), John Wiley and Sons, New York.

Basu, A., Brown, S.T., Christensen, J.N., DePaolo, D.J., Reimus, P.W., Heikoop, J.M., Woldegabriel, G., Simmons, G., Simmons, A.M., House, B.M., Hartmann, M., Maher, K., 2015. Isotopic and geochemical tracers for U(VI) reduction and U mobility at an *in situ* recovery U mine. Environ. Sci. Technol. 49, 5939-5947.

Ben Simon, R., Thiry, M., Schmitt, J.-M., Lagneau, V., Langlais, V., Bélières, M., 2014. Kinetic reactive transport modelling of column tests for uranium *In situ* Recovery (ISR) mining. Applied Geochem. 51, 116-129.

Borch, T., Roche, N., Johnson, T.E., 2012. Determination of contaminant levels and remediation efficacy in groundwater at a former *in situ* recovery uranium mine. J. Environ. Monit. 14, 1814-1823.

Bowell, R.J., Grogan, J., Hutton-Ashkenny, M., Broughm, C., Penman, K., Sapsford, D.J., 2011. Geometallurgy of uranium deposits Mater. Engineer. 24, 1305-1313.

Brown, S.T., Basu, A., Christensen, J.N., Reimus, P., Heikoop, J., Simmons, A., Woldegabriel, Maher, K., Weaver, K., Clay, J., DePaolo, D.J., 2016. Isotopic evidence for reductive immobilization of uranium across a roll-front mineral deposit. Environ. Sci. Technol. 50, 6189-6198.

Cai, C., Dong, H., Hongtao, L., Xiao, X., Ou, G., Zhang, C., 2007. Mineralogical and geochemical evidence for coupled bacterial uranium mineralization and hydrocarbon oxidation in the Shashagetai deposit, NW China. Chem. Geol. 236, 167-179.

Campbell, M.D., Wise, H.M., Rackely, R.I., 2007. Uranium in-situ leach development and associated environmental issues. Gulf Coast Assoc. Geol. Societies Trans. 57, 99-114.

Casas, I., de Pablo, J., Gimenez, J., Torrero, M.E., Bruno, J., Cera, E., Finch, R.J., Ewing, R.C., 1998. The role of pe, pH, and carbonate on the solubility of UO_2 and uraninite under nominally reducing conditions. Geochim. Cosmochim. Acta 62, 2223-2231.

Catchpole, G., Kucheka, R., 1993. Groundwater restoration in uranium ISL mines in the United States: Proceedings of Workshop on Uranium Production Environmental Restoration: An Exchange Between the United States and Germany: Hosted by USDOE UMTRA Project office, Albuquerque NM, pp. 294-302.

Cerrato, J.M., Ashner, M.N., Alessi, D.S., Lezama-Pacheco, J.S., Bernier-Latmani, R., Bargar, J.R., Giammar, D.E., 2013. Relative reactivity of biogenic and chemogenic uraninite and biogenic noncrystalline U(IV). Environ. Sci. Technol. 47, 9756-9763.

Chapelle, F.H., 1993. Ground-Water Geochemistry and Microbiology, John Wiley and Sons, New York.

Chapelle, F.H., Lovley, D.R., 1992. Competitive exclusion of sulfate-reduction by Fe(III)-reducing bacteria: A mechanism for producing discrete zones of high-iron groundwater. Ground Water 30, 29-36.

Chapelle, F.H., McMahon, P.B., Dubrovsky, N.M., Fujii, R.F., Oaksford, E.T., Vroblesky, D.A., 1995. Deducing the distribution of terminal electron accepting processes in hydrologically diverse groundwater systems. Water Resour. Res. 31, 359-371.

Clement, P., 2002. RT3D v2.5 Update Document.

Cuney, M., 2010. Evolution of uranium fractionation processes through time; Driving the secular variation of uranium deposit types. Econ. Geol. 105, 553-569.

Davis, J.A., Curtis, G.P., 2007. Consideration of geochemical issues in groundwater restoration at uranium in-situ leach mining facilities, U.S. Nuclear Regulatory Commission, NUREG/CR-6870, 86 pp.

Dershowitz, W., 2011. Discrete fracture network modeling in support of *in situ* leach mining. Mining Engineer. 2011, 48-50.

Descostes, M., Schlegel, M.L., Eglizaud, N., Descamps, F., Miserque, F., Simoni, E., 2010. Uptake of uranium and trace elements in pyrite (FeS_2) suspensions. Geochim Cosmochim. Acta, 74, 1551–1562.

Deutsch, W.J., Bell, N.E., Mercer, B.W., Serne, R.J., Shade, J.W., Tweeton, D.R., 1984. Aquifer restoration techniques for *in situ* leach uranium mines, NUREG/CR-3104; PNL-4583RU, 68 pp.

Deutsch, W.J., Martin, W.J., Eary, L.E., Serne, R.J., 1985. Methods of minimizing ground-water contamination from *in situ* leach uranium mines, NUREG/CR-3709, PNL-5319RU, 167 pp.

Devoto, R.H., 1978. Uranium in Phanerozoic sandstone and volcanic rock, in Short course in uranium deposits; their mineralogy and origin. American Geological Institute, Short Course Handbook 3, pp. 293-305.

DHI-WASY, 2013. FEFLOW 6.2 Finite Element Subsurface Flow and Transport Simulation System User Manual.

DOE, 1995. Decommissioning of US Uranium Production Facilities, USDOE, Energy Information Administration; Office of Coal, Nuclear, Electric and Alternative Fuels, DOE/EIA-0592, 71 pp.

Dong, W., Brooks, S.C., 2006. Determination of the formation constants of ternary complexes of uranyl and carbonate with alkaline earth metals (Mg^{2+}, Ca^{2+}, Sr^{2+}, and Ba^{2+}) using anion exchange method. Environ. Sci. Technol. 40, 4689-4695.

Duff, M.C., Coughlin, J.U., Hunter, D.B., 2002. Uranium co-precipitation with iron oxides. Geochim. Cosmochim. Acta 66, 3533-3547.

Dzombak, D.A., Morel, F.M.M., 1990. Surface Complexation Modeling: Hydrous Ferric Oxide, John Wiley and Sons, New York.

Fanghanel, T., Neck, V., 2002. Aquatic chemistry and solubility phenomena of actinide oxides/hydroxides. Pure Appl. Chem. 74, 1895-1907.

Finch, R.J., Ewing, R.C., 1992. The corrosion of uraninite under oxidizing conditions. J. Nuc. Mater. 190, 133-156.

Finch, W.I., Davis J.F., 1985. Sandstone-type uranium deposits--An introduction: IAEA TECDOC-328, pp. 11-20.

Gallegos, T.J., Campbell, K.M., Zielinski, R.A., Reimus, P.W., Clay, J.T., Janot, N., Bargar, J.R., Benzel, W.M., 2015. Persistent U(IV) and U(VI) following in-situ recovery (ISR) mining of a sandstone uranium deposit, Wyoming, USA. Applied Geochem. 63, 222-234.

Federal Register (2015). Environmental Protection Agency 40 CFR Part 192 Health and Environmental Protection Standards for Uranium and Thorium Mill Tailings; Proposed Rule, Volume 80, Number 16 (January 26, 2015). Available at: https://www.gpo.gov/fdsys/pkg/FR-2015-01-26/pdf/2015-00276.pdf.

Ford, R.G., Wilkin, R.T., Acree, S., 2008. Site characterization to support use of Monitored Natural Attenuation for remediation of inorganic contaminants in ground water. EPA Ground Water Issue Paper, EPA/600/R-08/114, 15 pp.

Galloway, W.E., 1978. Uranium mineralization in a coastal-plain fluvial aquifer system: Catahoula Formation, Texas. Econ. Geol. 73, 1655–1676.

Gershey, E.L., Klein, R.C., Party, E., Wilkerson, A., 1990. Low-level radioactive wastes, Van Nordstrom, New York.

Giblin, A.M., Batts, B.D., Swaine, D.J., 1981. Laboratory simulation studies of uranium mobility in natural waters. Geochim. Cosmochim. Acta 45, 699-709.

1113 Goldberg, S., 2014. Modeling selenate adsorption behavior on oxides, clay minerals, and soils
1114 using the triple layer model. Soil Science 179, 568-576.
1115
1116 Goldhaber, M.B., Reynolds, R.L., Rye, R.O., 1978. Origin of a south Texas roll-type uranium
1117 deposit: II. Sulfide petrology and sulfur isotope studies. Econ. Geol. 73, 1690-1705.
1118
1119 Gorman-Lewis, D., Mezeina, L., Fein, J.B., Szymanowski, J.E.S., Burns, P.C., Navrotsky, A.,
1120 2007. Thermodynamic properties of soddyite from solubility and calorimetry measurements. J.
1121 Chem. Thermodynamics 39, 568-575.
1122
1123 Gorman-Lewis, D. Shvareva, T., Kubatko, K.A., Burns, P.C., Wellman, D.M., McNamara, B.,
1124 Szymanowski, J.E.S., Navrotsky, A., Fein, J., 2009. Thermodynamic properties of autunite,
1125 uranyl hydrogen phosphate, and uranyl orthophosphate from solubility and calorimetric
1126 measurements. Environ. Sci. Technol. 43, 7416-7422.
1127
1128 Granger, H.C., Warren, C.G., 1969. Unstable sulfur compounds and the origin of roll-type
1129 uranium deposits. Econ. Geol. 64, 160-171.
1130
1131 Guillaumont, R., Fanghänel, T., Fuger, J., Grenthe, I., Neck, V., Palmer, D.A., Rand, M.H.,
1132 2003. Chemical Thermodynamics 5, Update on the Chemical Thermodynamics of Uranium,
1133 Neptunium, Plutonium, Americium and Technetium. Nuclear Energy Agency, OECD, Elsevier,
1134 Amsterdam.
1135
1136 Guo, L., Warnken, K.W., Santschi, P.H., 2007. Retention behavior of dissolved uranium during
1137 ultrafiltration: implications for colloidal U in surface waters. Mar. Chem. 107, 156-166.
1138
1139 Gwo, J.P., D'Azevedo, E.F., Frenzel, H., Mayes, M., Yeh, G.-T., Jardine, P.M., Salvage, K.M.,
1140 Hoffman, F.M., 2001. HBGC123D: a high-performance computer model of coupled
1141 hydrogeological and biogeochemical processes. Computers and Geosciences 27, 1231–1242.
1142
1143 Hall, S., 2009. Groundwater restoration at uranium in-situ recovery mines, south Texas coastal
1144 plain, US Geological Survey Open File Report 2009–1143, 32 pp.
1145
1146 Hall, S., 2014. World uranium resources, supply, and demand: Presentation at Energy from the
1147 Earth, A Congressional Briefing Series, March 11, 2014.
1148
1149 Harbaugh, A.W., 2005. MODFLOW-2005, the U.S. Geological Survey modular ground-water
1150 model -- the Ground-Water Flow Process, U.S. Geological Survey Techniques and Methods 6-
1151 A16.
1152
1153 Harshman, E.N., 1972. Geology and uranium deposits, Shirley Basin area, Wyoming. U.S.
1154 Geological Survey Professional Paper 745, 82 pp.
1155
1156 Harshman, E.N., 1974. Distribution of Some Elements in Some Roll-Type Uranium Deposits,
1157 Formation of Uranium Ore Deposits. Vienna, Austria. International Atomic Energy Agency,
1158 pp. 169–183.

Harshman, E.N., Adams, S.S., 1980. Geology and recognition criteria for roll-type uranium deposits in continental sandstones: Prepared for U.S.D.O.E under contract DE-AC13-76GJ01664, Publication GJBX-1(81), 181 pp.

Hobday, D. K., Galloway, W. E., 1999. Groundwater processes and sedimentary uranium deposits. Hydrogeol. J. 7, 127–138.

Huerta-Diaz, M.A., Morse, J.W., 1992. Pyritization of trace metals in anoxic marine sediments. Geochim. Cosmochim. Acta 56, 2681-2702.

HydroGeoLogic, 1996. MODHMS/MODFLOW-SURFACT Software Documentation.

Hyun, S.P., Davis, J.A., Sun, K., Hayes, K.F., 2012. Uranium(VI) reduction by iron(II) monosulfide mackinawite. Environ. Sci. Technol. 46, 336-3376.

IAEA, 2009. World distribution of uranium deposits (UDEPO) with uranium deposit classification: IAEA-TECDOC-1629, 117 pp.

Jang, J.H., Dempsey, B.A., Burgos, W.D., 2006. Solubility of schoepite: comparison and selection of complexation constants for U(VI). Water Res. 40, 2739-2746.

Johnson, R.H., Yoshino, M.E., Hall, S.M., Shea, V.M., 2010. Predictive Modeling Strategies for Operations and Closure at Uranium In-Situ Recovery Mines, *in* Wolkersdorfer, C., and Freund, A. (eds), Mine Water Innovative Thinking: Proceedings of the International Mine Water Association Symposium, 2010 Cape Breton University Press, Sydney, Nova Scotia, Canada, pp. 475-478.

Johnson, R.H., Diehl, S.F., Benzel, W.M., 2013. Solid-phase data from cores at the proposed Dewey-Burdock uranium in-situ recovery mine, near Edgemont, South Dakota. USGS OFR 2013-1093, 13 pp.

Kesler, S.E., 1994. Mineral Resources, Economics, and the Environment, MacMillan College Publishing Co., New York.

Krauskopf, K.B., 1988. Radioactive Waste Disposal, Chapman Hall, London.

Kyser, K., 2014. Uranium ore deposits, *in* S.D. Scott (ed.), Treatise of Geochemistry (2nd edition), Volume 13, Geochemistry of Mineral Deposits (Elsevier, Amsterdam), pp. 489–513.

Kyser, K., Cuney, M., 2008. Sandstone-hosted uranium deposits: Mineralogical Association of Canada, Short Course Series 39, pp. 221-240.

Langmuir, D., 1997. Aqueous Environmental Geochemistry, Prentice-Hall, Upper Saddle River, NJ.

Langmuir, D., 1978. Uranium solution-mineral equilibria at low temperatures with applications to sedimentary ore deposits. Geochim. Cosmochm. Acta 42, 547-569.

Larson, W.C., 1981. *In situ* leach mining—Current operations and production statistics, U.S. Bureau of Mines Information Circular no. 8852, pp. 3-7.

Lee, M.-K., Saunders, J.A., 2003. Effects of pH on metals precipitation and sorption: Field Bioremediation and geochemical modeling approaches. Vadose Zone J. 2, 177-185.

Leibold, J., 2013. Geochemistry and mineralogy of the alteration halo associated with the Three Crow roll-front uranium deposit, Nebraska, US, Unpublished Ph.D. Thesis, Colorado School of Mines, 173 pp.

Long, P.E., Yabusaki, S.B., Meyer, P.D., Murray, C.J., N'Guessan, A.L., 2008. Technical basis for assessing uranium bioremediation performance, NURG/CR-6973, 128 pp.

Lovley, D.R., 1991. Dissimilatory Fe(III) and Mn(IV) reduction. Microbiol. Reviews 55, 259–287.

Lovley, D.R., Phillips, E.J., 1988. Novel mode of microbial energy metabolism: organic carbon oxidation coupled to dissimilatory reduction of iron or manganese. Applied Environ. Microbiol. 54, 1472-1480.

Lovley, D.R.; Phillips, E.J.P.; Gorby, Y.A., Landa, E.R., 1991. Microbial reduction of uranium. Nature 350, 413-416.

Lovley, D.R., Roden, E.E., Phillips, E.J.P., Woodward, J.C., 1993. Enzymatic iron and uranium reduction by sulfate-reducing bacteria. Mar. Geol. 113, 41-53.

Ludwig, K.R., 1978. Uranium-daughter migration and U/Pb isotope apparent ages of uranium ores, Shirley Basin, Wyoming. Econ. Geol. 73, 29-49.

Ludwig, R.D., Su, C., Lee, T.R., Wilkin, R.T., Acree, S.D., Ross, R.R., Keeley, A., 2007. *In situ* chemical reduction of Cr(VI) in groundwater using a combination of ferrous sulfate and sodium dithionite: A field investigation. Environ. Sci. Technol. 41, 5299-5305.

Mann, D.K, Wong, G.T.F., 1993. Strongly bound uranium in marine waters: occurrence and analytical problems. Mar. Chem. 42, 25-37.

Marshall, T.A., Morris, K., Law, G.T.W., Livens, F.R., Mosselmans, J.F.W., Bots, P., Shaw, S., 2014. Environ. Sci. Technol. 48, 3724-3731.

Mehta, V.S., Maillot, F., Wang, Z., Catalano, J.G., Giammar, D.E., 2015. Transport of U(VI) through sediments amended with phosphate to induce *in situ* uranium immobilization. Water Res. 69, 307-317.

1251 Min, M.Z., Chen, J., Wang, J.P., Wei, G.H., Fayek, M., 2005a. Mineral paragenesis and textures
1252 associated with sandstone-hosted roll-front uranium deposits, NW China. Ore Geology Reviews
1253 26, 51–69.
1254
1255 Min, M.Z., Xu, M.H., Chen, J., Fayek, M., 2005b. Evidence of uranium biomineralization in
1256 sandstone-hosted roll-front uranium deposits, northwestern China. Ore Geology Reviews 26,
1257 198–206.
1258
1259 Moyes, L.N., Parkman, R.H., Charnock, J.M., Vaughan, D.J., Livens, F.R., Hughes, C.R.,
1260 Braithwaite, A., 2000. Uranium uptake from aqueous solution by interaction with goethite,
1261 lepidocrocite, muscovite, and mackinawite: An X-ray absorption spectroscopy study. Environ.
1262 Sci. Technol. 34, 1062-1068.
1263
1264 Mudd, G.M., 2001. Critical review of acid in-situ leach uranium mining: 1—USA and Australia.
1265 Environ. Geol. 41, 390–403.
1266
1267 Mukherjee, J., Ramkumar, J., Chandramouleeswaran, S., Shukla, R., Tyagi, A., 2013. Sorption
1268 characteristics of nano manganese oxide: efficient sorbent for removal of metal ions from
1269 aqueous streams. J. Radioanalytical Nuclear Chem. 297, 49-57.
1270
1271 Murowchick, J.B., Barnes, H.L., 1986. Marcasite precipitation from hydrothermal solutions.
1272 Geochim. Cosmochim. Acta 50, 2615-2629.
1273
1274 Murphy, M.J., Froehlich, M.B., Fifield, L.K., Turner, S.P., Schaefer, B.F., 2015. *In-situ*
1275 production of natural ^{236}U in groundwaters and ores in high-grade uranium deposits. Chem.
1276 Geol. 410, 213-222.
1277
1278 Nash, J.T., Granger, H.C., Adams, S.S., 1981. Geology and concepts of genesis of important
1279 types of uranium deposits, in B.J. Skinner (ed.), 75th Anniversary Volume, Econ. Geol. 1905-
1280 1980, pp. 63-116.
1281
1282 Nico, P.S., Stewart, B.D., Fendorf, S., 2009. Incorporation of oxidized uranium into Fe
1283 (hydr)oxides during Fe(II) catalyzed remineralization. Environ. Sci. Technol. 43, 7391-7396.
1284
1285 Niswonger, R.G., Panday, S., Ibaraki, M., 2011. MODFLOW-NWT, A Newton formulation for
1286 MODFLOW-2005, U.S. Geological Survey Techniques and Methods 6-A37, 44 pp.
1287
1288 Nuclear Regulatory Commission (NRC), 2003. Standard Review Plan for *In situ* Leach Uranium
1289 Extraction License Applications, Final Report. U.S. Nuclear Regulatory Commission, Office of
1290 Nuclear Material Safety and Safeguards, Washington, DC. NUREG-1569.
1291
1292 Nuclear Regulatory Commission (NRC). 2009a. Generic Environmental Impact Statement for
1293 In-Situ Leach Uranium Milling Facilities, Chapters 1 through 4, Final Report. U.S. Nuclear
1294 Regulatory Commission, Office of Federal and State Materials and Environmental Management
1295 Programs; and Wyoming Department of Environmental Quality, Land Quality Division.
1296 NUREG-1910, Vol. 1.

Nuclear Regulatory Commission (NRC), 2009b. Generic Environmental Impact Statement for In-Situ Leach Uranium Milling Facilities, Chapters 5 through 12 and Appendices A through G, Final Report. U.S. Nuclear Regulatory Commission, Office of Federal and State Materials and Environmental Management Programs; and Wyoming Department of Environmental Quality, Land Quality Division. NUREG-1910, Vol. 2.

Osiensky, J.L., Williams, R.E., 1990. Factors affecting efficient aquifer restoration at *in situ* uranium mine sites. Ground Water Monitoring and Remediation 10, 107-112.

Panday, S., Langevin, C.D., Niswonger, R.G., Ibaraki, M., Hughes, J.D., 2013. MODFLOW-USG version 1: An unstructured grid version of MODFLOW for simulating groundwater flow and tightly coupled processes using a control volume finite-difference formulation, U.S. Geological Survey Techniques and Methods, 66 pp.

Parkhurst, D.L., Kipp, K.L., Charlton, S.R., 2010. PHAST Version 2—A program for simulating groundwater flow, solute transport, and multicomponent geochemical reactions, U.S. Geological Survey Techniques and Methods 6–A35, 235 pp.

Pastukhov, A.M., Rychkov V.N., Smirnov, A.L., Skripchenko, S.Y., Poponin, N.A., 2014. Purification of *in situ* leaching solution for uranium mining by removing solids from suspension. Minerals Engin. 55, 1-4.

Pollock, D.W., 1994. User's Guide for MODPATH/MODPATH-PLOT, Version 3: A particle tracking post-processing package for MODFLOW, the U.S. Geological Survey finite-difference ground-water flow model, U.S. Geological Survey Open-File Report 94-464.

Pope, D.F., Acree, S.D., Levine, H., Mangion, S., van Ee, J., Hurt, K., Wilson, B., 2004. Performance monitoring of MNA remedies for VOCs in ground water, EPA/600/R-04/027.

Prat, O., Vercouter, T., Ansoborlo, E., Fichet, P., Perret, P., Kurttio, P., Salonen, L., 2009. Uranium speciation in drinking water from drilled wells in southern Finland and its potential links to health effects. Environ. Sci. Technol. 43, 3941-3946.

Pugliese, J.M., Larson, W.C., 1989. Uranium *in situ* mining research by the United States Bureau of Mines-A review, in *In situ* leaching of uranium: technical, environmental, and economic aspects, IAEA TECDOC-492, pp. 37-62.

Rackley, R. I., 1972. Environment of Wyoming Tertiary uranium deposits. American Assoc. Petrol. Geol. Bulletin 56, 755-774.

Rackley, R. I., 1976. Origin of western-states type uranium mineralization, *in* Handbook of strata-bound and stratiform ore deposits: Wolf, H.K. (ed.), Elsevier Scientific Publishing Co., Amsterdam, pp. 89-156.

Reynolds, R.L., Goldhaber, M.B., 1983. Iron disulfide minerals and the genesis of roll-type uranium deposits. Econ. Geol. 78, 105-120.

Reynolds, R.L., Goldhaber, M.B., Carpenter, D.J., 1982. Biogenic and nonbiogenic ore-forming processes in the south Texas uranium district: Evidence from the Panna Maria deposit. Econ. Geol. 77, 541-556.

Rickard, D., Luther, II, G.W., 1997. Kinetics of pyrite formation by the H_2S oxidation of iron (II) monosulfide in aqueous solutions between 25 and 125°C: The mechanism. Geochim. Cosmochim. Acta, 61, 135-147.

Rojas, J.L., 1989. Introduction to *in situ* leaching of uranium, *in In situ* leaching of uranium: technical, environmental, and economic aspects, IAEA TECDOC-492, pp. 7-20.

Rubin, B., 1970. Uranium roll front zonation in the southern Powder River Basin, Wyoming. Wyoming Geological Association Bulletin (December), pp. 5-12.

Saunders, J.A, Lee, M-K., Wolf, L.A., Morton, C.M., Feng, Y., Thomson, I., Park, S, 2005. Geochemical, microbiological, and geophysical assessments of anaerobic immobilization of heavy metals. Bioremediation J. 9, 33-48.

Saunders, J.A., Lee, M.-K., Shamsudduha, M., Chawdry, T., Ahmed, K.M., 2008. Geochemistry and mineralogy of arsenic under anaerobic conditions. Applied Geochem. 23, 3205-3214.

Saunders, J.A., Pritchett, M.A., Cook, R.B., 1997. Geochemistry of biogenic pyrite and ferromanganese stream coatings: A bacterial connection? Geomicrobiol. J. 14, 203-217.

Scott, T.B., Allen, G.C., Heard, P.J., Randell, M.G., 2005. Reduction of U(VI) to U(IV) on the surface of magnetite. Geochim. Cosmochim. Acta 69, 5639-5646.

Scott, T.B., Tort, O.R., Allen, G.C., 2007. Aqueous uptake of uranium onto pyrite surfaces; reactivity of fresh versus weathered material. Geochim. Cosmochim. Acta 71, 5044–5053.

Smedley, P.L., Kinniburgh, D.G., 2002. A review of the source, behavior and distribution of arsenic in natural waters. Applied Geochem. 17, 517-568.

Smith, M.E, 2011. Uranium mill closure in the USA: A historical perspective. Engineering Mining J. 211, 70-71.

Southam, G., Saunders, J.A., 2005. Geomicrobiology of ore deposits. Econ. Geol. 100, 1067-1084.

Staub, W.P., Hinkle, N.E., Williams, R.E., Anastasi, F., Osiensky. J., Rogness, D., 1986. An analysis of excursions at selected *in situ* uranium mines in Wyoming and Texas, ORNL/TM-9956 (NUREG/CR-3967), 296 pp.

1388 Stover, D.E., 2004. Smith Ranch ISL uranium facility: The well field management program:
1389 Recent developments in uranium resources and production with emphasis on *in situ* leach
1390 mining, IAEA TECDOC-1396, pp. 189-203.
1391
1392 Tang, G., Wu, W.-M., Watson, D.B., Parker, J.C., Schadt, C.W., Shi, X., Brooks, S.C., 2013.
1393 U(VI) bioreduction with emulsified vegetable oil as the electron donor – microcosm tests and
1394 model development. Environ. Sci. Technol. 47, 3209-3217.
1395
1396 Tani, Y., Ohashi, M., Miyata, N., Seyama, H., Iwahori, K., Soma, M., 2004. Sorption of Co(II),
1397 Ni(II), and Zn(II) on biogenic manganese oxides produced by a Mn-oxidizing fungus, strain
1398 KR21-2. J. Environ. Sci. Health A Tox. Hazard. Subst. Environ. Eng. 39, 2641-2460.
1399
1400 Troyer, L.D., Tang, Y., Borch, T., 2014. Simultaneous reduction of arsenic(V) and uranium(VI)
1401 by mackinawite: role of uranyl arseante precipitate formation. Environ Sci. Technol. 48, 14326-
1402 14334.
1403
1404 U.S. Environmental Protection Agency (EPA), 1995. Extraction and beneficiation of ores and
1405 minerals, Volume 5: Uranium, EPA 530-R-94-032, NTIS PB94-2008987, 139 pp.
1406
1407 U.S. Environmental Protection Agency (EPA), 2007a. Monitored Natural Attenuation of
1408 Inorganic Contaminants in Groundwater, Vol. 1: Technical Basis for Assessment, EPA/600/R-
1409 07/139, 94 pp.
1410
1411 U.S. Environmental Protection Agency (EPA), 2007b. Monitored Natural Attenuation of
1412 Inorganic Contaminants in Groundwater, Vol. 2: Assessment for Non-Radionuclides Including
1413 Arsenic, Cadmium, Chromium, Copper, Lead, Nickel, Nitrate, Perchlorate, and Selenium,
1414 EPA/600/R-07/140, 124 pp.
1415
1416 U.S. Environmental Protection Agency (EPA), 2008. A Systematic Approach for Evaluation of
1417 Capture Zones at Pump and Treat Systems, EPA/600/R08/003.
1418
1419 U.S. Environmental Protection Agency (EPA), 2010. Monitored Natural Attenuation of
1420 Inorganic Contaminants in Groundwater, Vol. 3: Assessment for Radionuclides Including
1421 Tritium, Radon, Strontium, Technetium, Uranium, Iodine, Radium, Thorium, Cesium, and
1422 Plutonium-Americium, EPA/600/R-10/093, 147 pp.
1423
1424 U.S. Environmental Protection Agency (EPA), 2014. Goliad Aquifer Exemption – Request for
1425 Public Comment Fact Sheet. Available at:
1426 http://www.epa.gov/region6/water/swp/groundwater/goliad-aquifer/goliad-factsheet.pdf
1427
1428 Underhill, D.H., 1992. In-Situ Leach Uranium Mining in the United States of America: Past,
1429 Present and Future, In "Uranium *In situ* Leaching", Proceedings of a Technical Committee
1430 Meeting, Vienna, Austria, October 5-8, 1992, IAEA TECDOC-720, 23 pp.
1431
1432 Walton, A.W., Galloway, W.E., Henry, C.D., 1981. Release of uranium from the volcanic glass
1433 in sedimentary sequences: An analysis of two systems. Econ. Geol. 76, 69-88.

Wang, X., Xu, S., Zhang, B., Zhao, S., 2011. Deep-penetrating geochemistry for sandstone-type uranium deposits in the Turpan–Hami basin, north-western China. Applied Geochem. 26, 2238-2246.

Wang, Y., Feng, X., Villalobos, M., Tan, W., Liu, F., 2012. Sorption behavior of heavy metals on birnessite: Relationship with its Mn average oxidation state and implications for types of sorption sites. Chem. Geol. 292-293, 25-34.

Ward, J.R., 1983. Well design and construction for *in situ* leach uranium extraction. Ground Water Monitoring and Remediation 3, 79-83.

Watson, D.B., Wu. W.-M., Mehlhorn, T., Tang, G., Earles, J., Lowe, K., Gihring, T.M., Zhang, G., Phillips, J., Boyanov, M.I., Spalding, B.P., Schadt, C., Kemner, K.M., Criddle, C.S., Jardine, P.M., Brooks, S.C., 2013. In situ bioremediation of uranium with emulsified vegetable oil as the electron donor. Environ. Sci. Technol. 47, 6440-6448.

Way, S.C., 2008. Well-field mechanics for in-situ uranium mining: Southwest Hydrology, Nov./Dec. 2008, pp. 30-31.

WoldeGabriel, G., Boukhalfa, H., Ware, S.D., Chesire, M., Reimus, P., Heikoop, J., Conradson, S.D., Batuk, O., Havrilla, G., House, B., Simmons, A., Clay, J., Basu, A., Christensen, J.N., Brown, S.T., DePaolo, D.J., 2014. Characterization of cores from an in-situ recovery mined uranium deposit in Wyoming: Implications for post-mining restoration. Chem. Geol. 390, 32-45.

World Nuclear Association, 2014. *In situ* leach (ISL) mining of uranium: WNA website, http://www.world-nuclear.org/info/Nuclear-Fuel-Cycle/Mining-of-Uranium/In-Situ-Leach-Mining-of-Uranium/.

Wu, W.-M., Carley, J., Gentry, T., Ginder-Vogel, M.A., Fienen, M., Mehlhorn, T., Yan, H., Carrol, S., Pace, M.N., Nyman, J., Luo, J., Gentile, M.E., Fields, M.W., Hickey, R.F., Gu, B., Watson, D., Cirpka, O.A., Zhou, J., Fendorf, S., Kitanidis, P.K., Jardine, P., Criddle, C.S., 2006. Pilot-scale in situ bioremediation of uranium in a highly contaminated aquifer. 2. Reduction of U(VI) and geochemical control of U(VI) bioavailability. Environ. Sci. Technol. 40, 3986-3995.

Xu, T., Sonnenthal, E., Spycher, N., Pruess, K., 2006. TOUGHREACT: A simulation program for non-isothermal multiphase reactive geochemical transport in variably saturated geologic media: Applications to geothermal injectivity and CO_2 geological sequestration. Comput. Geosci. 32, 145-165.

Yi, Z.J., Tan, K.X., Tan, A.L., Yu, Z.X., Wang, S.Q., 2007. Influence of environmental factors on reductive bioprecipitation of uranium by sulfate reducing bacteria. Intern. Biodet. Biodegrad. 60, 258-266.

Zachara, J.M., Long, P.E., Bargar, J., Davis, J.A., Fox, P., Fredrickson, J.K., Freshley, M.D., Konopka, A.E., Liu, C., McKinley, J.P., Rockhold, M.L., Williams, K.H., Yabusaki, S.B., 2013.

Persistence of uranium groundwater plumes: contrasting mechanisms at two DOE sites in the groundwater-river interaction zone. J. Contam. Hydrol. 147, 45-72.

Zheng, 2010. MT3DMS v5.3 Supplemental User's Guide, Department of Geological Sciences, The University of Alabama.

Zyvoloski, 2007. FEHM: A control volume finite element code for simulating subsurface multi-phase multi-fluid heat and mass transfer, LA-UR-3359. May.

Table 1

Principal minerals reported in roll-front uranium deposits from the USA (compiled from Devoto, 1978; Harshman and Adams, 1980; Nash et al., 1981; and Bowell et al., 2011).

Uraninite	UO_2 (crystalline)
Pitchblende	UO_2 (amorphous)
Coffinite	$U(SiO_4)_{0.9}(OH)_{0.4}$
Carnotite	$K_2(UO_2)_2(VO4)_2 \cdot 3H_2O$
Native selenium	Se
Native sulfur	S
Ferroselite	$FeSe_2$
Pyrite	FeS_2
Marcasite	FeS_2
Mackinawite	FeS
Molybdenite	MoS_2 (crystalline)
Jordisite	MoS_2 (amorphous)
Haggite	$V_2O_2(OH)_3$
Doloresite	$H_8V_6O_{16}$
Paramontroseite	VO_2
Montroseite	$(V^{3+},Fe^{3+})O(OH)$
Hematite	Fe_2O_3
Goethite	FeOOH
Siderite	$FeCO_3$
Gypsum	$CaSO_4 \cdot 2H_2O$
Calcite	$CaCO_3$
Kaolinite	$Al_2Si_2O_5(OH)_4$
Montmorillonite	$(Na,Ca)_{0.33}(Al,Mg)_2(Si_4O_{10})(OH)_2 \cdot nH_2O$

Table 2

Selected water quality data for baseline and post-restoration conditions for uranium *in situ* recovery sites in the USA.

Parameter	EPA MCL[a]	Mean Baseline Condition	Mean Post-Restoration Condition[b]	Site	Reference
Arsenic (µg/L)	10	<20	335	--	1
		1	30	Highland, WY	2, 3
		2	24	Crow Butte, NE	2
		<5	30	Ruth, WY	2
Selenium (µg/L)	50	<10	790	--	1
		1	70	Highland, WY	2, 3
		3	1	Crow Butte, NE	2
		20	<10	Ruth, WY	2
Molybdenum (µg/L)	3.7[c]	100	100	Highland, WY	2, 3
		69	<100	Crow Butte, NE	2
		<50	<10	Ruth, WY	2
Vanadium (µg/L)	180[c]	<50	330	--	1
		100	100	Highland, WY	2, 3
		66	260	Crow Butte, NE	2
		50 as V_2O_5	120 as V_2O_5	Ruth, WY	2
Manganese (µg/L)	50[d]	30	490	Highland, WY	2, 3
		110	10	Crow Butte, NE	2
		10	150	Ruth, WY	2
Iron (µg/L)	300[d]	50	1300	Highland, WY	2, 3
		44	<50	Crow Butte, NE	2
		<10	470	Ruth, WY	2
Uranium (µg/L)	30	50	5280	--	1
		50	3530	Highland, WY	2, 3
		92	963	Crow Butte, NE	2
		10 as U_3O_8	410 as U_3O_8	Ruth, WY	2
Radium-226 (pCi/L)	5[e]	21.6	>100	--	1
		675	1153	Highland, WY	2, 3
		229.7	246.7	Crow Butte, NE	2
		55	41	Ruth, WY	2
Sulfate (mg/L)	250[c]	159	252	--	1
		91	127.2	Highland, WY	2, 3
		356	287	Crow Butte, NE	2
		104	91	Ruth, WY	2
Chloride (mg/L)	250[c]	4.7	18	Highland, WY	2, 3
		204	124	Crow Butte, NE	2
		6	7.5	Ruth, WY	2

Notes: [a]MCL is EPA's Maximum Contaminant Level for drinking water sources. [b]At Highland (WY) >15 pore volumes were replaced using groundwater sweep, reverse osmosis, and reductive recirculation. At Crow Butte (NE) ~19 pore volumes were removed and 16.4 pore volumes were recirculated. [c]EPA Groundwater Protection Screening Level. [d]Secondary MCL. [e]MCL is for combined Ra-228 plus Ra-226.

References: [1]Anastasi and Williams (1984); [2]Davis and Curtis (2007); [3]Borch et al. (2012).

List of Figures

Figure 1. Map showing locations of principal sandstone-hosted uranium districts of the western US, and operating ISR mines (and three additional ones licensed and under construction as of 2014). Modified from U.S. EPA (1995) and Hall (2014).

Figure 2. (a) Eh-pH diagram for U at 25°C; system U-O-H-C-Ca with $\Sigma U=10^{-5}$, $\Sigma Ca=10^{-3}$, and $PCO_2=10^{-2.5}$ bar (uraninite = UO_2; schoepite = β-$UO_3 \cdot 2H_2O$). (b) Solubility of U^{+4} as uraninite and amorphous UO_2 as a function of pH. (c) Solubility of U^{+6} as a function of pH at various levels of PCO_2 and at $aH_4SiO_4=10^{-4.0}$ (soddyite = $(UO_2)_2SiO_4 \cdot 2H_2O$). Schoepite solubility is also shown from data of Jang et al. (2006). (d) Solubility of U^{+6} as a function of pH in the presence of phosphate (10^{-4} molal; autinite = $Ca(UO_2)_2(PO_4)_2 \cdot 3H_2O$) and at various levels of PCO_2 and calcium (10^{-3} molal). Thermodynamic data used for the construction of these diagrams were from Langmuir (1997), Guillaumont et al. (2003), Jang et al. (2006), and Gorman-Lewis et al. (2007, 2009). The EPA maximum contaminant level (MCL) for uranium in drinking water is plotted for reference (30 µg/L).

Figure 3. Diagrammatic cross section showing geology, mineralogy, and geochemistry of a typical roll-front uranium deposit. Compiled from Devoto (1978), Harshman (1972, 1974), Harshman and Adams (1980), and Nash et al. (1981). Geochemistry largely reflects that of the Shirley Basin, WY deposits, although Mo data are from southeast Texas ores. Scale shown is approximate.

Figure 4. Backscatter scanning electron microscope (SEM) image of uranium ore from the Dewey-Burdock prospect, South Dakota showing uranium and vanadium minerals, along with more common detrital quartz, feldspar grains, and interstitial calcite (from Johnson et al., 2013; see Fig. 1 for location).

Figure 5. Diagrammatic cross section of geochemical zonation of a confined aquifer due to common geomicrobiologic controls, also showing approximate conditions where uranium will precipitate due to reduction (after Southam and Saunders, 2005).

Figure 6. Example of a network design for performance monitoring, including target zones for monitoring effectiveness with respect to specific remedial objectives. In this example, monitoring network design is based on transects of wells oriented perpendicular to the groundwater flow direction. Sampling locations for target monitoring zones were chosen based on site characterization. Piezometers provide additional data for evaluation of changes in potential groundwater flow direction (from Pope et al., 2004).

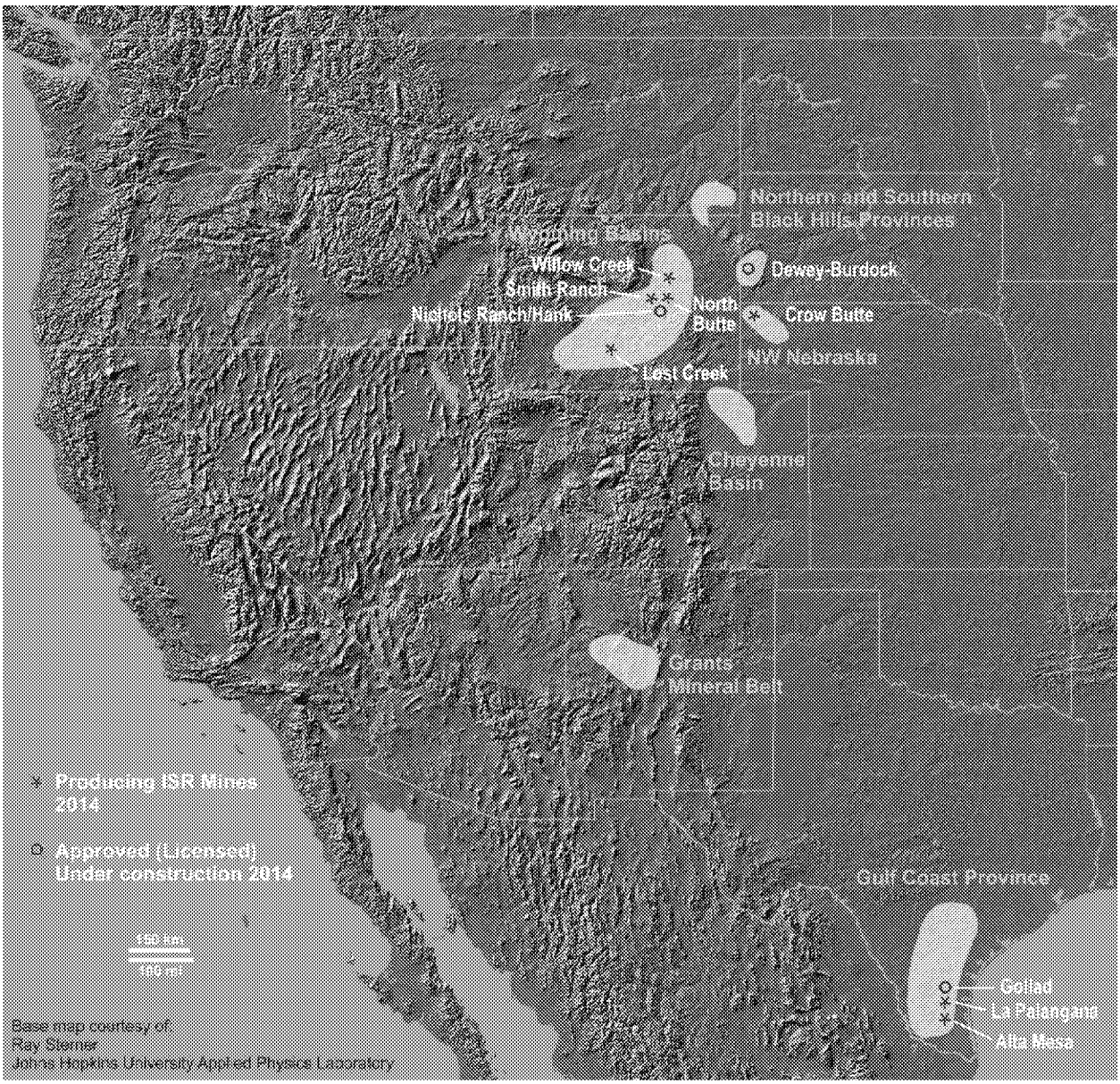
Northern and Southern
Black Hills Provinces
Powder River Basin
Willow Creek
Smith Ranch
Nichols Ranch/Hank
Dewey-Burdock
North
Butte
Crow Butte
NW Nebraska
Lost Creek
Cheyenne
Basin
Grants
Mineral Belt
Producing ISR Mines
2014
Approved (Licensed)
Under construction 2014
Gulf Coast Province
Goliad
La Palangana
Alta Mesa
Base map courtesy of:
Ray Sterner
Johns Hopkins University Applied Physics Laboratory

Figure 1

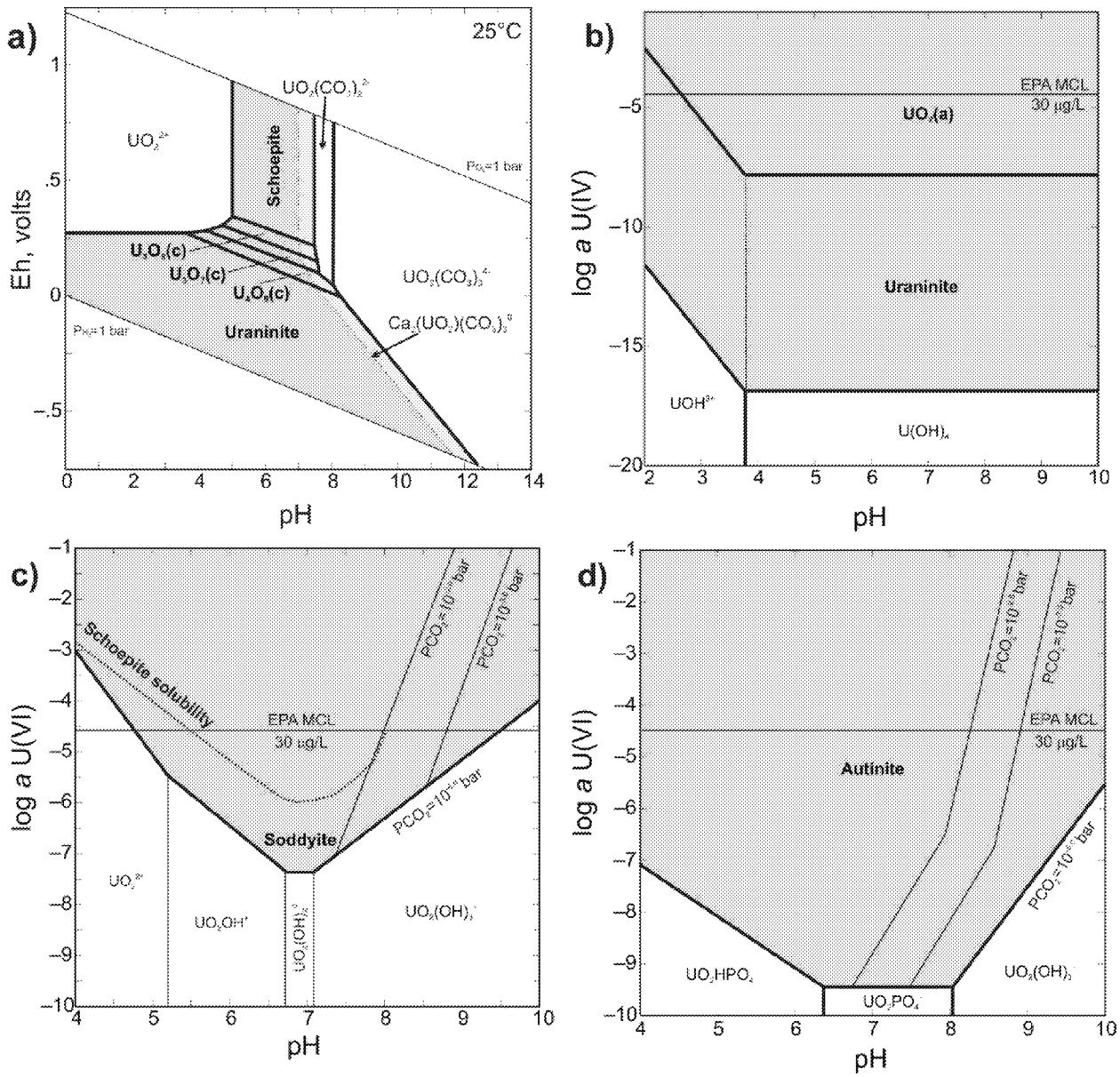
a)
25°C
Eh, volts
pH
UO_2^{2+}
$UO_2(CO_3)_2^{2-}$
Schoepite
P_{O_2}=1 bar
U_3O_8(c)
U_3O_7(c)
U_3O_4(c)
Uraninite
$UO_2(CO_3)_3^{4-}$
$Ca_2(UO_2)(CO_3)_3^0$
b)
log a U(IV)
EPA MCL
30 µg/L
UO_2(a)
Uraninite
UOH^{3+}
$U(OH)_4$
c)
log a U(VI)
Schoepite solubility
EPA MCL
30 µg/L
$PCO_2=10^{-1.5}$ bar
$PCO_2=10^{-3.5}$ bar
$PCO_2=10^{-2.0}$ bar
Soddyite
UO_2^{2+}
UO_2OH^+
$UO_2(OH)_2^0$
$UO_2(OH)_3^-$
d)
Autinite
UO_2HPO_4
$UO_2PO_4^-$
$UO_2(OH)_3^-$

Figure 2

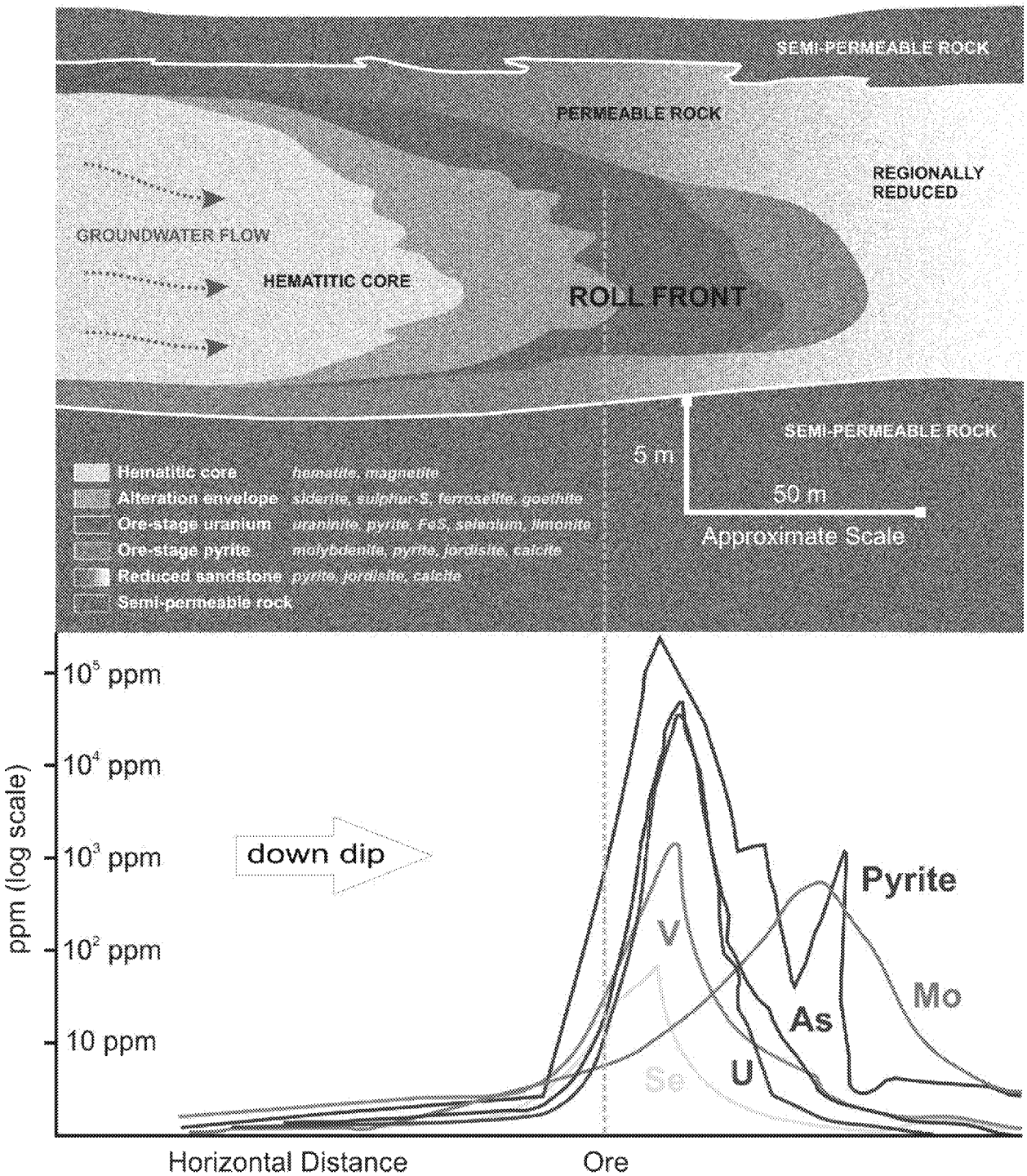
SEMI-PERMEABLE ROCK
PERMEABLE ROCK
REGIONALLY REDUCED
GROUNDWATER FLOW
HEMATITIC CORE
ROLL FRONT
SEMI-PERMEABLE ROCK
5 m
50 m
Approximate Scale
Hematitic core hematite, magnetite
Alteration envelope siderite, sulphur-S, ferroselite, goethite
Ore-stage uraninum uraninite, pyrite, FeS, selenium, limonite
Ore-stage pyrite molybdenite, pyrite, jordisite, calcite
Reduced sandstone pyrite, jordisite, calcite
Semi-permeable rock
ppm (log scale)
10^5 ppm
10^4 ppm
10^3 ppm
10^2 ppm
10 ppm
down dip
Pyrite
V
Mo
As
Se
U
Horizontal Distance
Ore

Figure 3

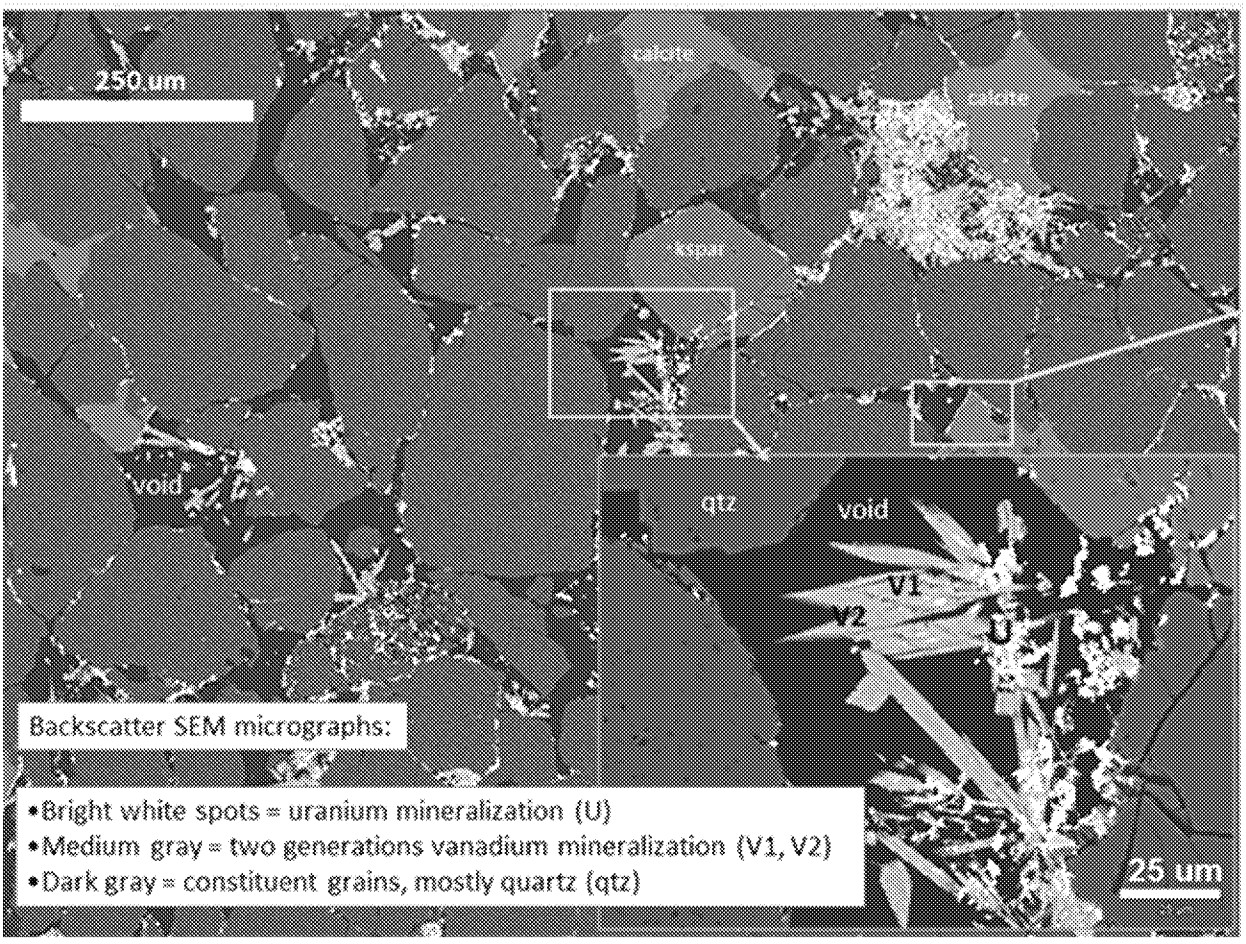
250 um
calcite
calcite
kaol
void
qtz
void
V1
V2
U
Backscatter SEM micrographs:
•Bright white spots = uranium mineralization (U)
•Medium gray = two generations vanadium mineralization (V1, V2)
•Dark gray = constituent grains, mostly quartz (qtz)
25 um

Figure 4

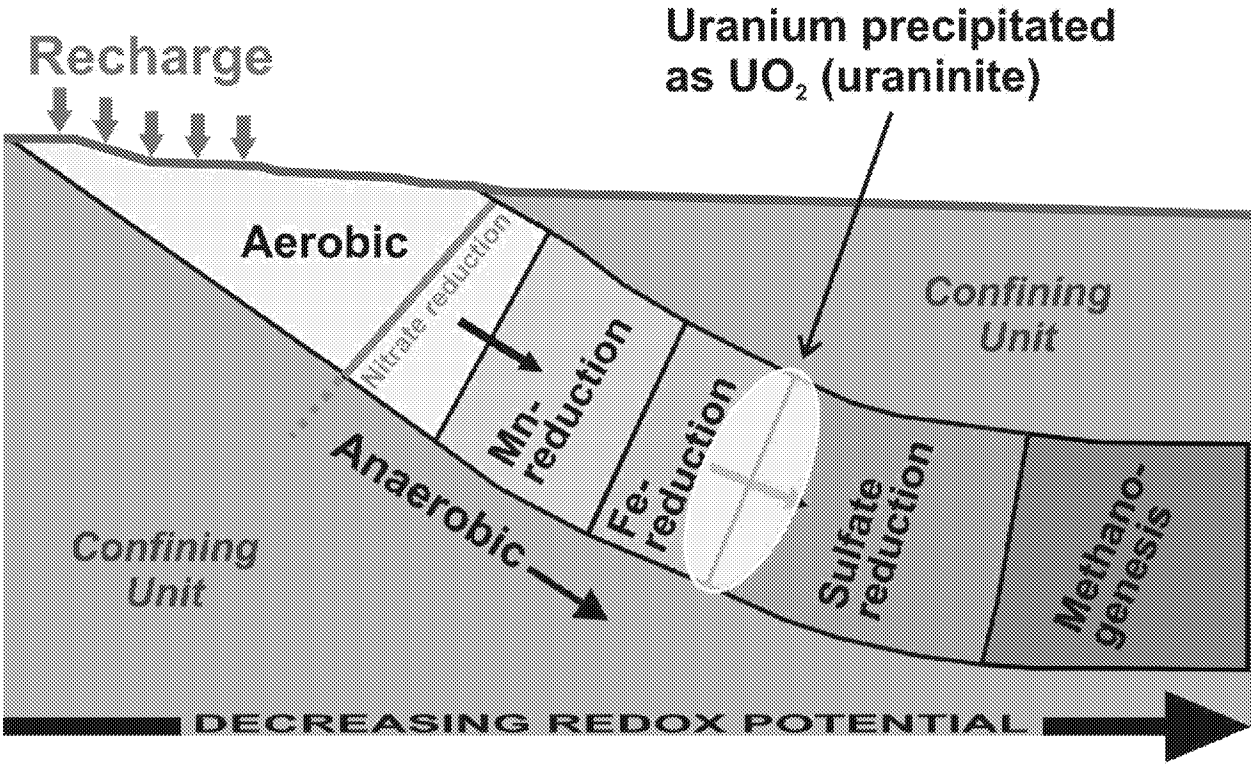
Recharge
Uranium precipitated as UO_2 (uraninite)
Aerobic
Nitrate reduction
Mn-reduction
Fe-reduction
Sulfate reduction
Methano-genesis
Anaerobic
Confining Unit
Confining Unit
DECREASING REDOX POTENTIAL

Figure 5

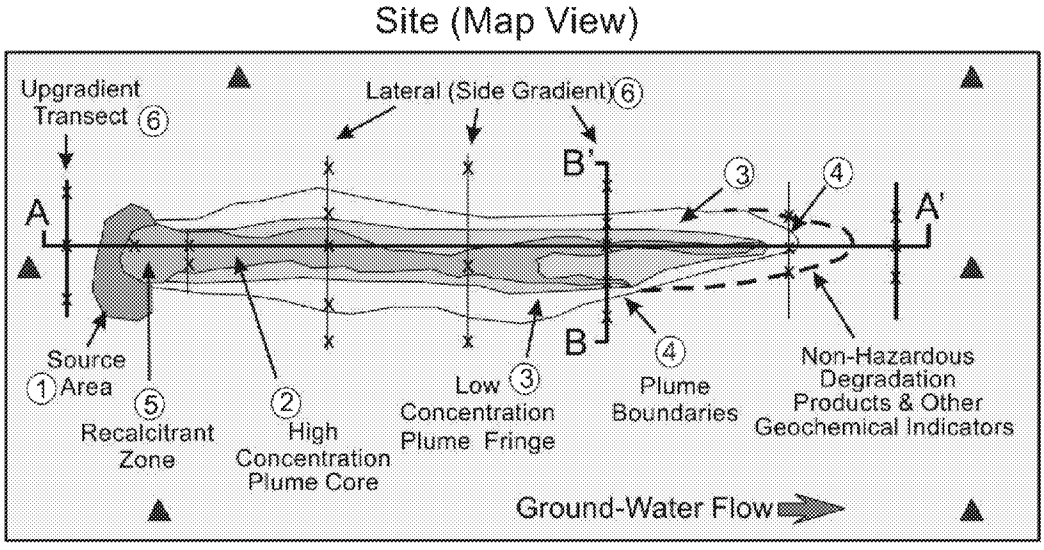

Target Monitoring Zones

1. Source area
2. Contaminated zones of highest concentrations and mobility
3. Plume fringes
4. Plume boundaries
5. Recalcitrant zone determined from historical trends
6. Upgradient and sidegradient locations

x Monitoring well cluster

▲ Piezometer

x–x–x Transect of well clusters

Figure 6